ELSEVIER
SAUNDERS

Neurosurg Clin N Am 18 (2007) 431–461

NEUROSURGERY
CLINICS
OF NORTH AMERICA

Postnatal Maturation and Radiology of the Growing Spine

Sharon E. Byrd, MD[a,b,*], Elizabeth M. Comiskey, MD[a,c]

[a]*Rush Medical College, 1653 West Congress Parkway, Chicago, IL 60612, USA*
[b]*Section of Neuroradiology, Department of Diagnostic Radiology and Nuclear Medicine, Rush University Medical Center, 1653 West Congress Parkway, Chicago, IL 60612, USA*
[c]*Section of Pediatric Radiology, Department of Diagnostic Radiology and Nuclear Medicine, Rush University Medical Center, 1653 West Congress Parkway, Chicago, IL 60612, USA*

The spine is part of the supporting framework of the body and is composed of vertebrae, discs, and ligaments. It continues to mature postnatally, with marked changes occurring predominantly in the vertebrae during infancy, childhood, and early adolescence. Maturation of the spine is not only manifested by the ossification process but by changes in the shape of the vertebrae, spinal curvature, spinal canal, discs, and bone marrow. The parts of the spine and the maturation process can be evaluated by various imaging modalities such as conventional plain spine imaging (CPSI [plain spine radiography]), CT, and MRI. CPSI is historically one of the best modalities for imaging the bony spine. CT provides better bone detail and allows finer evaluation of subtle structures, the soft tissue of the spine (discs, ligaments), and the spinal cord. MRI is not the modality of choice to demonstrate bone detail but it provides excellent resolution of the bone marrow, ligaments, and discs of the spine. MRI can be used as an adjunct for visualization of the soft tissue of the spine and intraspinal contents (Fig. 1) [1–4].

* Corresponding author. Section of Neuroradiology, Department of Diagnostic Radiology and Nuclear Medicine, Rush University Medical Center, 1653 West Congress Parkway, Chicago, IL 60612.
E-mail address: sebyrd7730@sbcglobal.net (S.E. Byrd).

Anatomy

The spine consists of osseous and soft tissue components that provide support and mobility for the body and a protective covering for the central nervous system. The vertebral column is composed of 7 cervical, 12 thoracic, and 5 lumbar vertebrae; the sacrum (composed of 5 fused vertebrae that become progressively smaller); and the coccyx (3 to 5 rudimentary vertebrae). A typical vertebra consists of a body and neural arch. The neural arch is composed of bilateral pedicles, laminae, superior and inferior articulating facets, transverse processes, and a unilateral spinous process. The vertebral body is composed of an outer rim of cortical bone and an inner matrix of cancellous bone, marrow, and fat (see Fig. 1). Some minor differences exist at segmental levels of the bony spine. The cervical vertebrae (from C1 to C6) have a foramen in each of their transverse processes called the foramen transversarium (for the vertebral arteries) (Fig. 2). The first and second cervical vertebrae are unique and differ considerably from the other cervical vertebrae. The first cervical vertebra (atlas) has the shape of a ring. It consists of anterior and posterior arches with paired lateral masses. The arches form in the midline. Each lateral mass consists of a transverse process with a foramen transversarium and superior (condylar fossa) and inferior articular facets (Fig. 3). The second cervical vertebra (axis) consists of the odontoid process (dens), body, lateral masses, laminae, and a spinous process. Each paired lateral mass consists

1042-3680/07/$ - see front matter
doi:10.1016/j.nec.2007.05.002

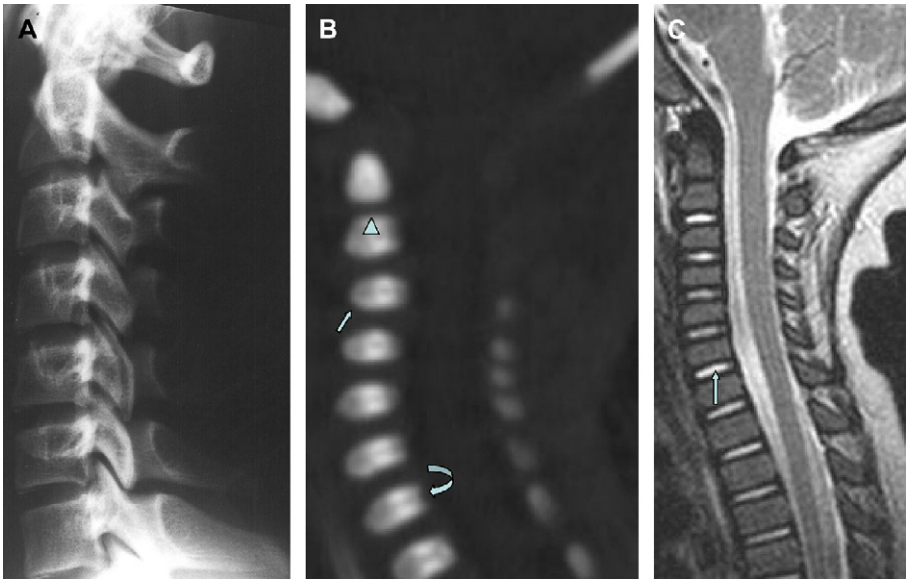

Fig. 1. Normal spine images. (*A*) Lateral CPSI in a 5-year-old demonstrating bone detail. (*B*) Sagittal reformatted CT (multiplanar reconstruction) of a 2-day-old demonstrating bone detail with oval-shaped ossification centers of vertebrae (*arrow*) with posterior channel for basivertebral vein (*curved arrow*) and subdental synchondrosis of C2 (*arrowhead*). (*C*) Sagittal MRI T2-W fast spin-echo in a 1-year-old showing bone marrow, hyperintense discs (*arrow*), and spinal cord.

of a pedicle, a foramen transversarium, and superior and inferior articular facets. The odontoid process consists of a tip (os terminale) and a body, which is connected to the main body of the axis at the subdental synchondrosis (Fig. 4). The thoracic vertebrae have costal facets for the rib attachments (see Fig. 2) [1–6].

Twenty-three intervertebral discs (IVDs) extend from the C2-3 to the L5-S1 intervertebral levels. No IVDs exist between the cranium and C1, between C1 and C2, in the sacrum, or in the coccyx. The IVD is composed of an outer fibrous tissue or fibrocartilage (the annulus fibrosus) and a central semiliquid gelatinous substance (the nucleus pulposus). The IVD is connected to the adjacent end plates of each vertebral body by its annulus fibrosus and is considered an amphiarthrosis, or half joint. The IVD becomes avascular after 4 to 5 years of age (Fig. 5) [1–15].

The other joints of the spine consist of the facet joints, the joints of Luschka, and the sacroiliac joints. The facets (apophyseal or zygapophyseal) are true synovial joints extending bilaterally from each vertebral level from C3 to S1, consisting of hyaline cartilage on the articular surfaces of the inferior articular facet of the superior vertebra to the superior articular facet of the inferior vertebra (Fig. 6) [1–15].

The joints of Luschka are not true synovial joints. They are bilateral articulation from C3 to C7 between the uncinate process of the superolateral margins of the vertebral body and the inferolateral margin of the above adjacent vertebral body. The joints of Luschka do not form until after 10 years of age when loose fibrous tissue in this area is reabsorbed, leaving a cleft that appears similar to an articulation. The sacroiliac joints are complex multiplanar articulations between the sacrum and pelvis. The costovertebral and costotransverse articulations are true synovial articulations between the ribs and vertebral bodies (costovertebral), and between the ribs and transverse processes. The craniocervical articulations are a complex set of synovial articulations that allow flexion, extension, and rotary motion of the head on the neck (see Fig. 6) [1–15].

The main ligaments of the spine are the anterior and posterior longitudinal ligaments running along the anterior and posterior surfaces of the vertebral bodies. The ligamentum flava join contiguous borders of adjacent laminae. The supraspinous and interspinous ligaments join adjacent spinous processes. The intertransverse ligaments join adjacent transverse processes (see Fig. 5) [1–15].

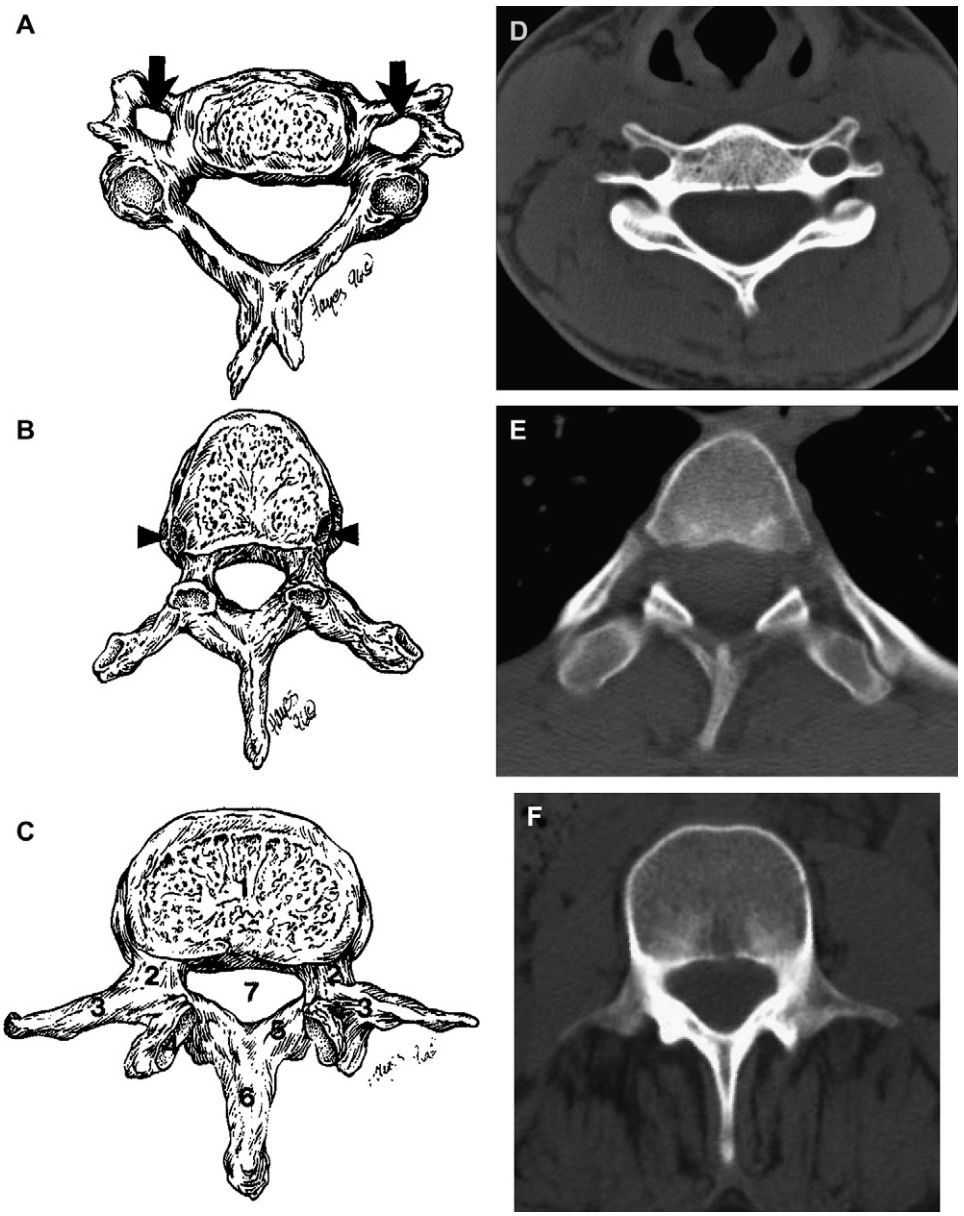

Fig. 2. Diagrams and CT scans of typical vertebra at each level. (*A* and *D*) Cervical vertebra diagram and CT axial with bilateral transverse foramina (*arrows in A*). (*B* and *E*) Thoracic vertebra diagram and CT axial with bilateral costal facets (*arrowheads in B*). (*C* and *F*) Lumbar vertebra diagram and CT axial; diagram shows body (*1*), pedicle (*2*), transverse process (*3*), superior articulating facet (*4*), lamina (*5*), spinal process (*6*), and spinal canal (*7*). (*From* McLone DG. Pediatric neurosurgery. 4th edition. Philadelphia: Saunders; 2001. p. 113; with permission [Fig. 2A–C].)

The major ligamentous attachments at the base of the skull, C1 and C2, consist of the anterior longitudinal ligament; the apical ligament (which extends from the tip of the dens to the tip of the clivus); the cruciform ligament (the transverse portion, which lies behind the tip of the dens between the inner aspect of the lateral masses of C1, and the vertical portion, which connects the body of the dens to the occiput); the posterior longitudinal ligament; the tectorial membrane (the

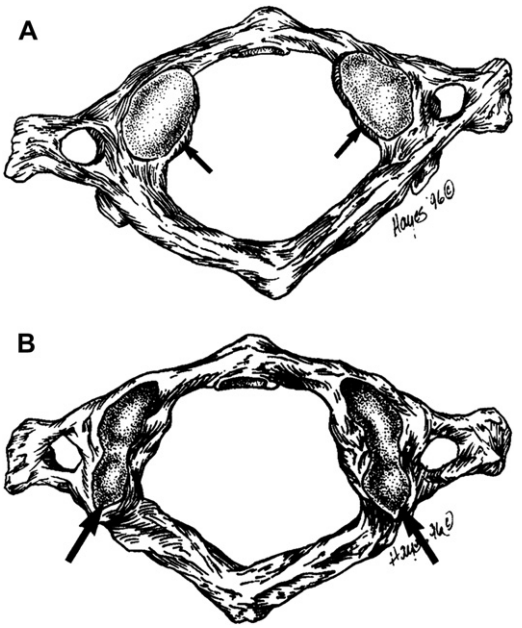

Fig. 3. C1 (atlas) vertebra: typical appearance. Superior surface (*A*) with condylar fossa (*short arrows*) for articulations with occipital condyles, and inferior surface (*B*) with inferior articulating facets (*long arrows*) for articulations with axis (C2). (*From* McLone DG. Pediatric neurosurgery. 4th edition. Philadelphia: Saunders; 2001. p. 113; with permission.)

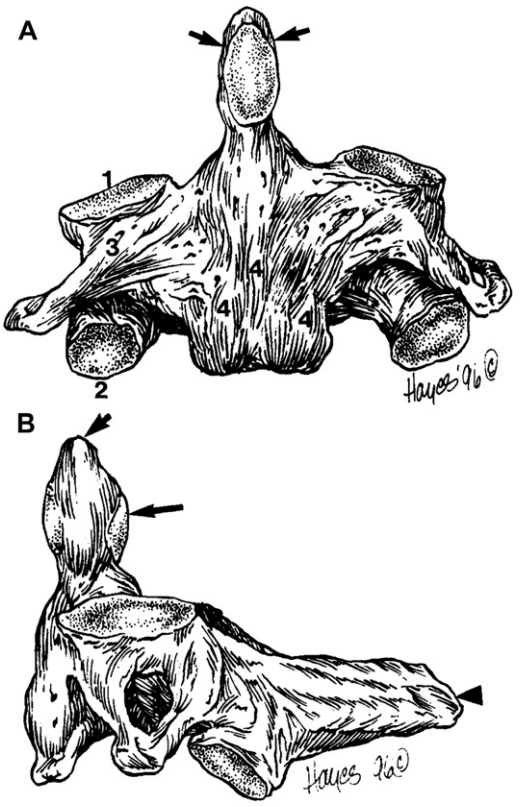

Fig. 4. C2 (axis) vertebra anterior view (*A*) with odontoid process (dens) (*short arrows*), superior (*1*) and inferior (*2*) articulating facets, transverse processes (*3*), and body of axis (*4*). Oblique lateral view (*B*) with tip (*small arrow*) and body (*large arrow*) of odontoid process and spinous process (*arrowhead*). (*From* McLone DG. Pediatric neurosurgery. 4th edition. Philadelphia: Saunders; 2001. p. 114; with permission.)

continuation of the posterior longitudinal ligament along the posterior border of the dens to the clivus); the atlantoaxial ligaments (which attach the body of C2 to the lateral masses of C1); the alar ligaments (which extend from the tip of the dens to the inferomedial aspects of the occipital condyles); the anterior atlantooccipital ligament (which is continuous with the anterior longitudinal ligament and extends from the anterior arch of C1 to the anterior portion of the foramen magnum ligamentum flavum at C1-C2); and the posterior atlantooccipital ligament analogous to the ligamentum flavum of the spine (which extends from the posterior arch of C1 to the posterior portion of the foramen magnum) (Fig. 7) [1–15].

The spinal canal is a bony tube lined with ligaments that contains primarily the spinal cord, spinal nerve roots, and cerebrospinal fluid. Its borders are anteriorly, the posterior aspect of the vertebral bodies, IVDs, and posterior longitudinal ligament; posteriorly, by the bony neural arch and ligamentum flavum; and laterally, by the pedicles and facet joints (see Fig. 5). It is round to oval in shape in the cervical, thoracic, and upper lumbar regions. It becomes triangular in appearance in the mid- and lower lumbar and sacral regions. In the young adult, the sagittal diameter of the spinal canal measures 15 to 27 mm in the lumbar, 17 to 22 mm in the thoracic, and 15 to 27 mm in the cervical region of the spine [1–15].

The intervertebral foramina are bilateral bony openings extending the length of the spine, containing the spinal nerve roots, vessels, and fat. They are oval in shape and increase in size as they extend inferiorly down the spine. They are bounded anteriorly by the vertebral bodies and IVD, above and below by the pedicles, and posteriorly by the superior and inferior articular facets and ligamentum flavum [1–15].

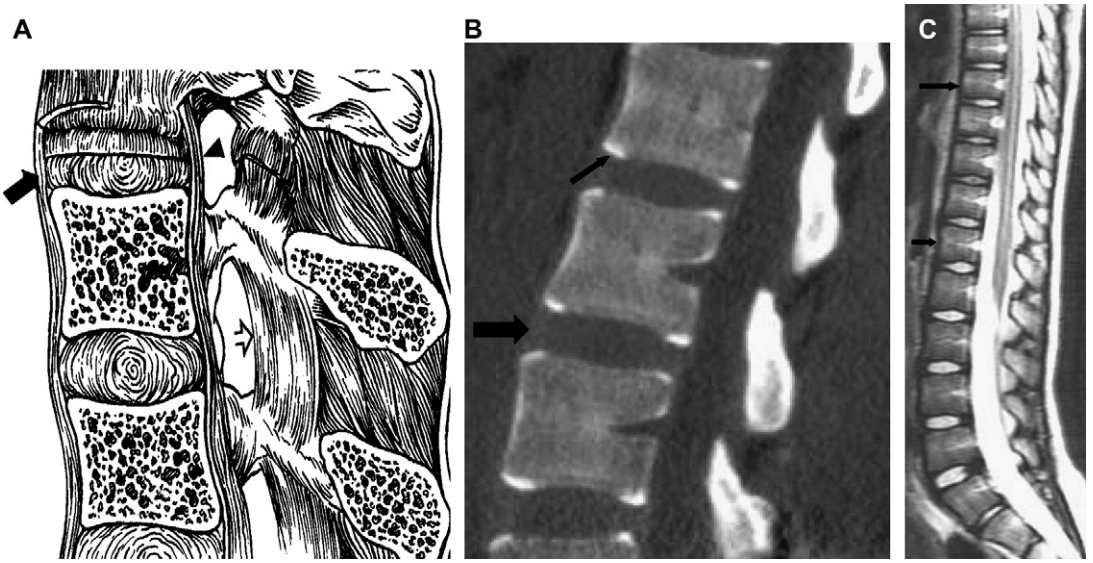

Fig. 5. IVDs and ligaments of the spine. (*A*) Lateral diagram of a segment of the upper lumbar spine with IVDs and ligamentous attachments: anterior (*closed arrow*) and posterior (*arrowhead*) longitudinal ligaments, ligamentum flavum (*open arrow*), and interspinous ligaments. (*From* McLone DG. Pediatric neurosurgery. 4th edition. Philadelphia: Saunders; 2001. p. 14; with permission.) (*B*) Sagittal multiplanar reconstruction CT of a 17-year-old upper lumbar spine. Vertebral body with ring apophysis increased density at end plates (*small arrow*) and isodense IVDs (*large arrow*). (*C*) Sagittal MRI T2-weighted image of an 11-year-old thoracolumbar spine with hypointense anterior longitudinal ligament (*arrows*).

Imaging modalities

Conventional plain spine imaging (plain spine radiography)

Various imaging modalities are available to evaluate the pediatric spine. CPSI is the initial modality of choice, with CT and MRI as adjuncts to define better the bone, soft tissue, or intraspinal contents. CPSI and CT use x-rays to create an image and thus are a form of radiation to the pediatric patient. Because CPSI uses ionizing radiation, care and experience are extremely important in obtaining adequate views. Initially, anterior-posterior (AP) and lateral views are obtained. Additional views, such as the lateral swimmers' view (to evaluate cervicothoracic junction), flexion and extension lateral views (to evaluate movement), oblique views, or views through the mouth AP (to evaluate atlas and axis) are obtained only depending on the history, the physical examination, or findings on the initial images (Fig. 8). Practices have changed and CT is now often used to evaluate the spine further, instead of obtaining some of these additional views (see Fig. 8).

The radiologic evaluation of CPSI consists of analyzing the soft tissues, alignment, vertebral bodies, posterior elements, spinal canal, and intervertebral (neural) foramina. All of the spine at each level should be visualized. For example, in evaluating the cervical spine, the craniocervical junction, C1 to C7, and the upper border of T1, should be seen. The prevertebral and paravertebral soft tissue symmetry, size, and delineation of normal planes are assessed. The prevertebral soft tissue of the cervical spine is best seen on the lateral view. The retropharyngeal space (between the posterior pharyngeal wall and the anterior-inferior margin of C2) should not be greater than 7 mm, with an average of 3.5 mm in children. The soft tissue space between the posterior tracheal wall and the anterior-inferior aspect of C6 should be less than 14 mm, with an average of 7 to 8 mm in children. Occasionally, a prevertebral fat stripe may be seen on the lateral view in children. This stripe is a thin radiolucent line adjacent to the anterior surface of the vertebrae, lying parallel to the anterior longitudinal ligament. These soft tissues planes can be seen not only on CPSI but also on CT and MRI (see Fig. 8). In the thoracic and lumbar spine, the paravertebral soft tissue is seen on the AP views. The soft tissue should be symmetric, with sharp planes [1–6,15].

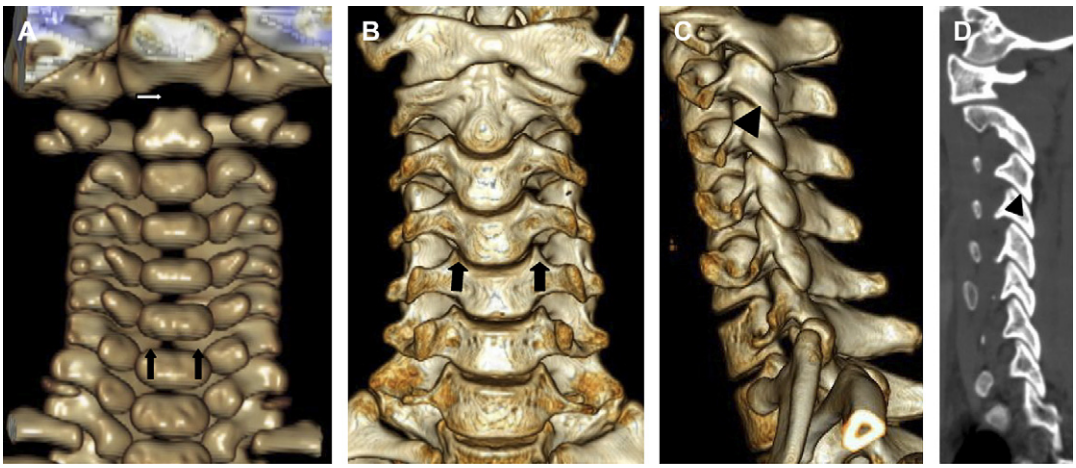

Fig. 6. (*A*) Three-dimensional volume rendering technique of anterior posterior view of cervical spine in a 2-day-old child; normally, the joints of Luschka (*black arrows*) and os terminale (*white arrow*) of C2 vertebra are not developed at this age. (*B*) Three-dimensional volume rendering technique of anterior posterior view of cervical spine in a 17-year-old with joints of Luschka (*large arrows*). (*C*) Three-dimensional volume rendering technique lateral view and (*D*) multiplanar reconstruction CT sagittal view of facet joints (*arrowheads*) of cervical spine in a 17-year-old.

The vertebrae should have normal alignment on all views. The spine should be straight on the AP view (Fig. 9). The normal lordotic curvature of the cervical and lumbar spine and the normal kyphosis of the thoracic and sacrococcygeal spine are seen on the neutral lateral view. Alignment of the spine is maintained by the ligaments, joints, vertebrae, discs, and adjacent musculature.

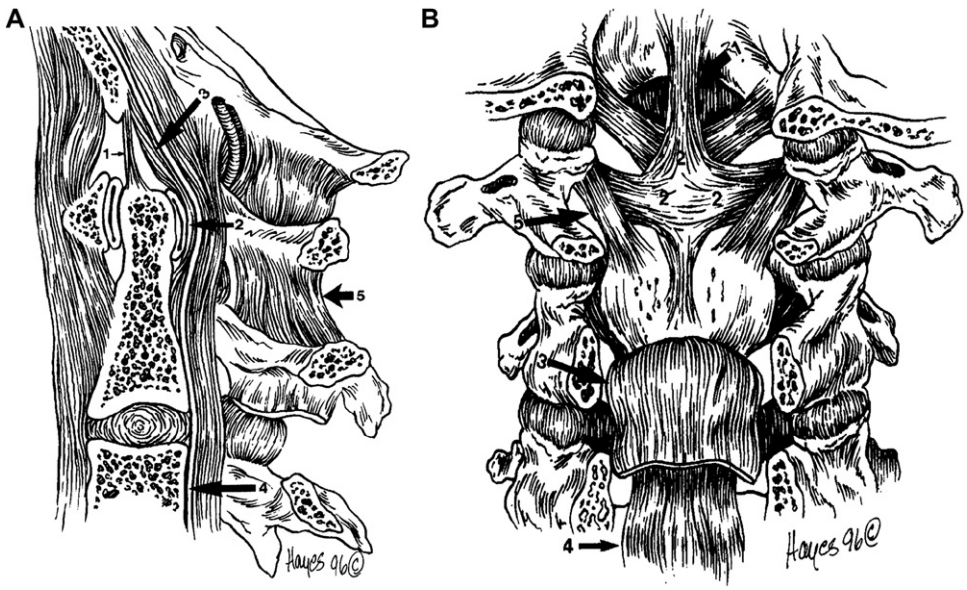

Fig. 7. (*A*) Lateral diagram of craniocervical junction with ligamentous attachments: apical (*1*), cruciate (*2*), tectorial membrane (*3*), posterior longitudinal (*4*), and spinous (*5*) ligaments. (*B*) Posterior-anterior diagram of ligaments at craniocervical junction with apical (*1*), vertical and transverse bands of cruciate (*2*), tectorial membrane (*3*), posterior longitudinal (*4*), and alar (*5*) ligaments. (*From* McLone DG. Pediatric neurosurgery. 4th edition. Philadelphia: Saunders; 2001. p. 115; with permission.)

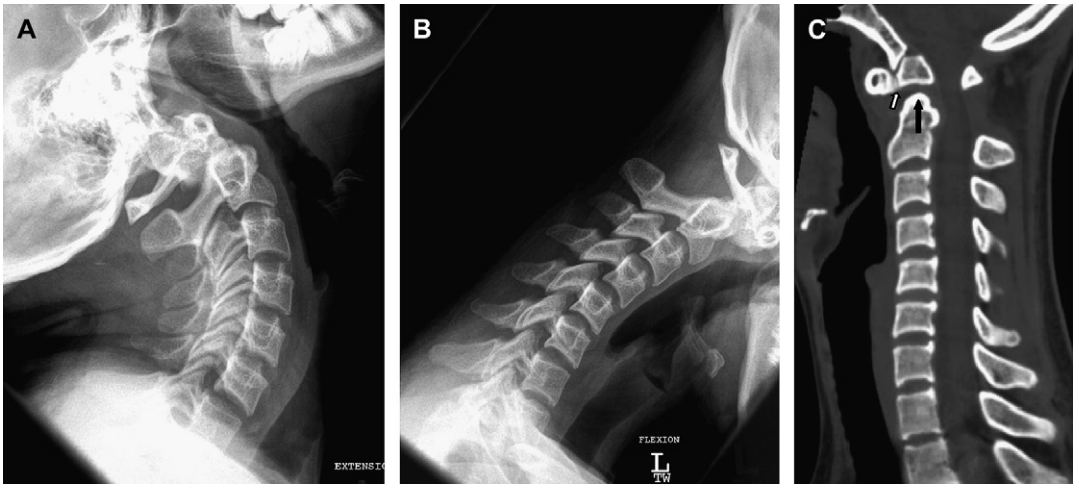

Fig. 8. CPSI lateral views in (*A*) extension and (*B*) flexion, and (*C*) multiplanar reconstruction CT sagittal in a 17-year-old with abnormal ununited os terminale of odontoid of C2 (os odontoideum) (*black arrow*) and fusion to body of C1 (*white arrow*).

Lordosis, kyphosis, and anterior and posterior subluxation are evaluated on the lateral views. Flexion and extension views may be necessary to evaluate abnormal movement of the spine. The degree of scoliosis, torticollis, and lateral subluxation is evaluated on AP views. The vertebra should align with those above and below. Imaginary lines can be seen, or lines drawn, on the CPSI images to connect parts of the spine to evaluate alignment. The most common lines are demonstrated on lateral views. The three lines are the anterior and posterior vertebral lines, and the laminar line connecting the laminae. These lines flow in gentle curves following the normal curvature of each specific level of the spine (Fig. 10). Straightening of the spine (loss of the normal curvature) on the lateral view is abnormal; some of the common causes are muscle spasm, trauma, infection, and poor posture [1–6,15].

Normal areas of pseudosubluxation can be seen on the lateral view. The most common locations of normal pseudosubluxation are in the cervical spine at C2-C3 and C3-C4 in young children and C4-5 or C5-6 in older children (Fig. 11). The C1-dens distance (atlantoaxial relationship between the posterior margin of the arch of C1 and the anterior margin of the odontoid process) should measure no more than 5 mm in children. This distance is usually between 3 and 5 mm in infants and young children, and can normally increase 1 to 2 mm on the flexion lateral view. Pseudospread of the lateral masses of C1 is a normal variant in infants, and could simulate a Jefferson fracture on AP views [1–6,15,16].

The vertebra (bodies and posterior elements), spinal canal, and neural foramina vary in appearance and size during the postnatal development of the spine. In general, in the older child, the vertebral bodies are rectangular in appearance. Unique vertebrae (C1, C2, sacrum, and coccyx) differ considerably in appearance from most vertebrae.

CT

CT is the next modality for evaluating the pediatric spine. CT is a computer-based noninvasive imaging modality that uses x-rays (ionizing radiation) to produce radiologic images in the axial, coronal, sagittal, or oblique planes. It provides the best bone detail, with some detail of the discs, paraspinal musculature, spinal cord, and nerve roots. State-of-the-art CT scanners can produce a submillimeter slice thickness image in less than a second. CT technology is based on a x-rays beam and detector system [17–21].

Introduced 30 years ago, CT has undergone breakthrough technology within the last 10 years, with the emergence of multislice CT (MSCT) scanners. One of the major advantages of MSCT is in postprocessing. MSCT, in comparison to single-slice CT, took a fundamental step from a cross-sectional view to a truly three-dimensional (3D) imaging modality that allows arbitrary cut

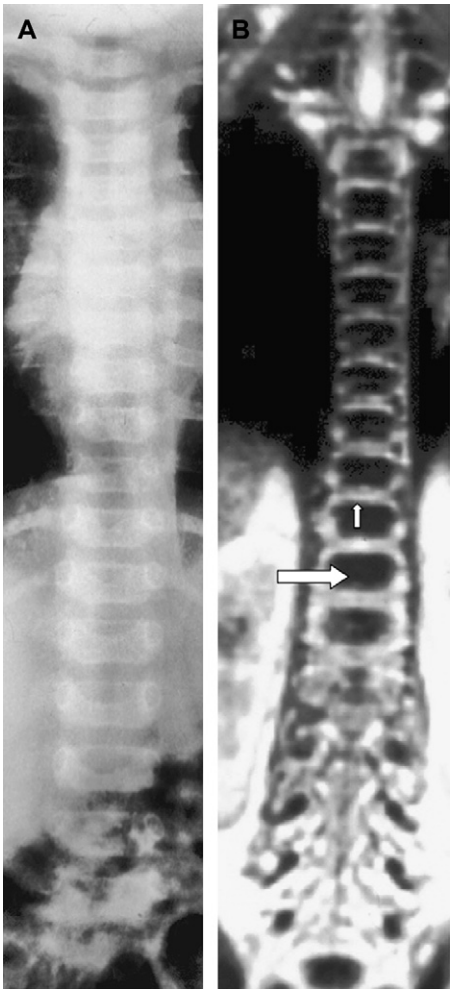

Fig. 9. (*A*) CPSI AP view with normal straight spine and paraspinal soft tissue planes in a 3-month-old child. (*From* McLone DG. Pediatric neurosurgery. 4th edition. Philadelphia: Saunders; 2001. p. 116; with permission.) (*B*) MRI T1-weighted coronal view with normal straight spine, hypointense bone marrow of the vertebral bodies (*large arrow*), and hyperintense cartilaginous end plates (*small arrow*) in a newborn.

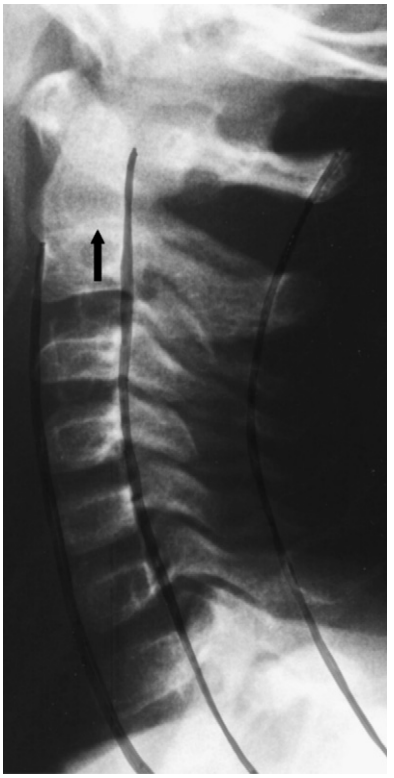

Fig. 10. Lateral cervical CPSI in a 3-year-old normal cervical spine with partial fusion (closing) of subdental synchondrosis (*arrow*), normal kyphosis curvature, and the three alignment lines (anterior, middle, and posterior).

planes and superb display of data sets. The newer generation of MSCT scanners allows near-isotropic voxel acquisitions, which is a prerequisite for delineation of highly detailed two-dimensional multiplanar reconstructions (MPR) and 3D reconstructed images (see Figs. 6 and 8). MSCT provides spine sections in the same image quality as the source. Any plane can be reformatted from the acquired volume. Three-dimensional postprocessing has different 3D rendering software packages. The two most common are the surface shaded display (SSD) and the volume rendering technique (VRT) (Figs. 12–14). SSD is capable of demonstrating gross 3D relationships but fails to display lesions hidden beneath the bone surface. The 3D VRT conveys more information than SSD and can show multiple internal and overlying features, such as the IVDs and ligaments and the bony vertebrae. One of the major disadvantages of MSCT is the increased radiation dose compared with conventional single-slice CT scanners; however, the radiation dose to the child can be significantly reduced by tailoring the image protocol (parameters) to the clinical question [17–21].

The spine is routinely scanned in the direct axial plane with the child supine. The x-ray beam is perpendicular to the long axis of the spine. With special software packages, the axial images can be postprocessed into coronal, sagittal, or oblique images with MPR, or into 3D images. The images are viewed with bone settings (high window and level settings) to evaluate bony detail and with soft

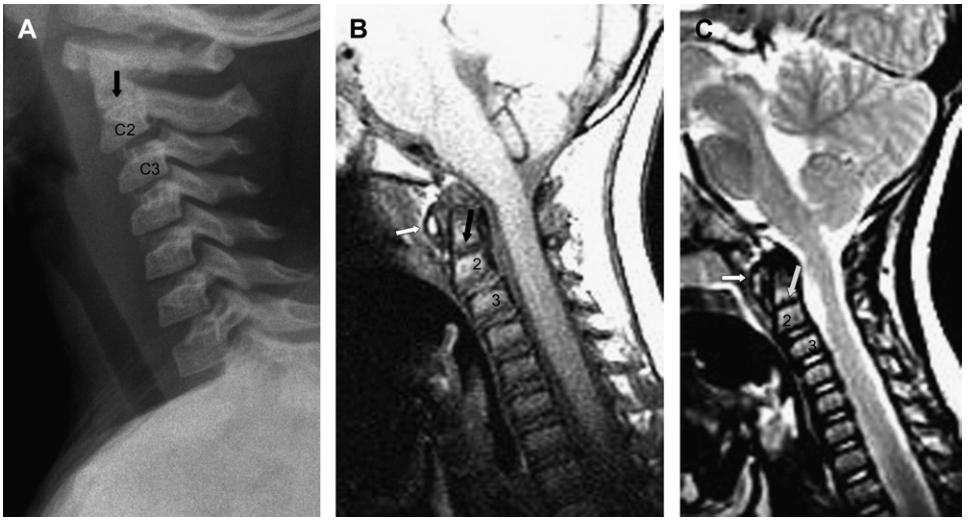

Fig. 11. (*A*) Lateral CPSI in a 2-year-old with normal pseudosubluxation C2-C3 and incompletely ossified subdental synchondrosis of C2 (*black arrow in A and B and large white arrow in C*). (*B*) MRI T1-weighted and (*C*) fast spin-echo T2-W in a 5-year-old with normal pseudosubluxation at C2-C3 and cartilaginous body of C1 (*small white arrow*).

tissue settings to evaluate discs, ligaments, spinal cord, nerve roots, and paraspinal muscles. In the infant and very young child, the discs and other soft tissue components are not well demonstrated (see Figs. 12–14). CT studies are routinely performed without intravenous iodinated contrast material. To evaluate the dura or soft tissue abnormalities of the spine, contrast may be required [17–21].

The anatomy demonstrated on the CT study of the spine is the routine spine anatomy, with bone anatomy and pathology being well demonstrated. Although soft tissue components such as bone marrow, discs, ligaments, spinal cord, nerve roots,

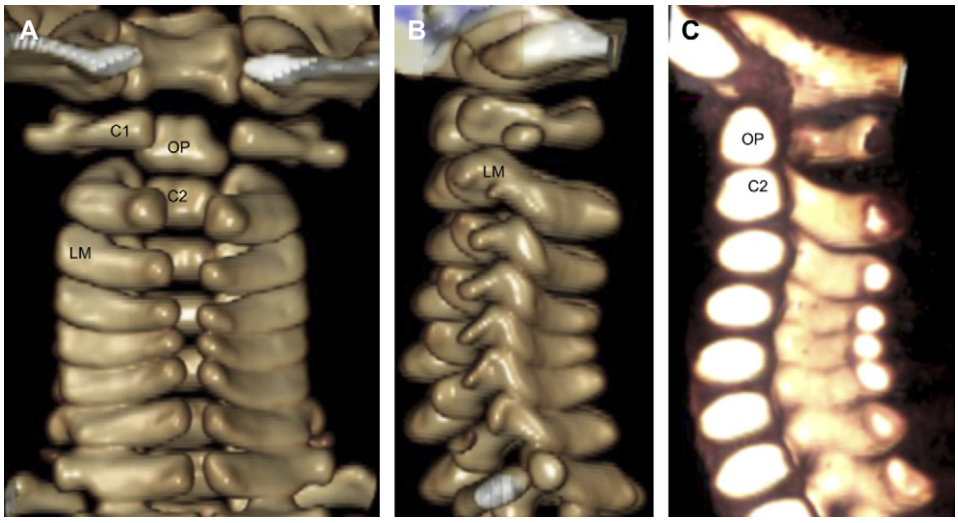

Fig. 12. 3D VRT images of 2-day-old cervical spine. (*A*) Posterior-anterior view with nonossified os terminale of odontoid process (*OP*), body of C2, lateral masses of vertebrae (*LM*) and nonossified laminae/spinous processes. (*B*) 3D VRT lateral view. (*C*) Midline section of the lateral view of 3D VRT with non visualization of body of C1 due to ossification centers not developed at this age, odontoid process (OP) and body of C2 ossification centers, cervical vertebral bodies demonstrate oval shaped ossification centers, as well as, ossification centers demonstrated in posterior elements of these cervical vertebrae.

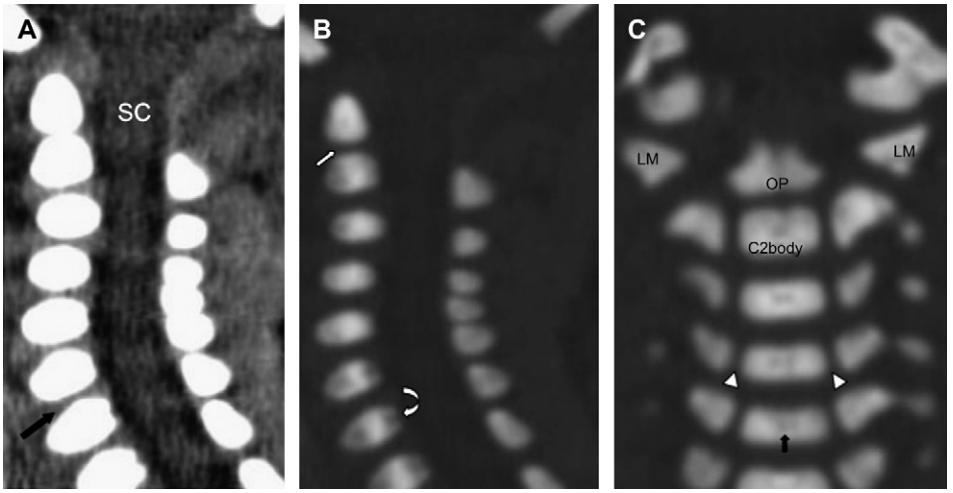

Fig. 13. CT of a 2-day-old newborn. (*A*) MPR sagittal soft tissue settings with spinal cord (*SC*), discs (*arrow*). (*B*) MPR sagittal bone settings with dense ossification centers of bodies and posterior elements of vertebrae, nonossified subdental synchondrosis of C2 (*small white arrow*), and posterior channel for basivertebral vein (*curved arrow*). (*C*) MPR coronal bone settings. No os terminale, not ossified, nonossified neurocentral synchondrosis at junction of bodies with lateral masses of vertebrae (*arrowheads*), C2 (body) and odontoid process (*OP*), channel for basivertebral vein (*black arrow*), C1 lateral masses (*LM*).

and paraspinal muscles are demonstrated on CT, these structures are better defined on MRI.

MRI

MRI is a computer-based imaging method that uses radio waves and a strong magnetic field to generate an image of the tissues and organs of the body. The contraindications to an MRI examination consist of various pacemakers, some aneurysmal clips, and any metal in the eye. MRI is the modality of choice in evaluating intraspinal pathology. It can be used as an adjunct in further evaluating bony abnormalities in children to

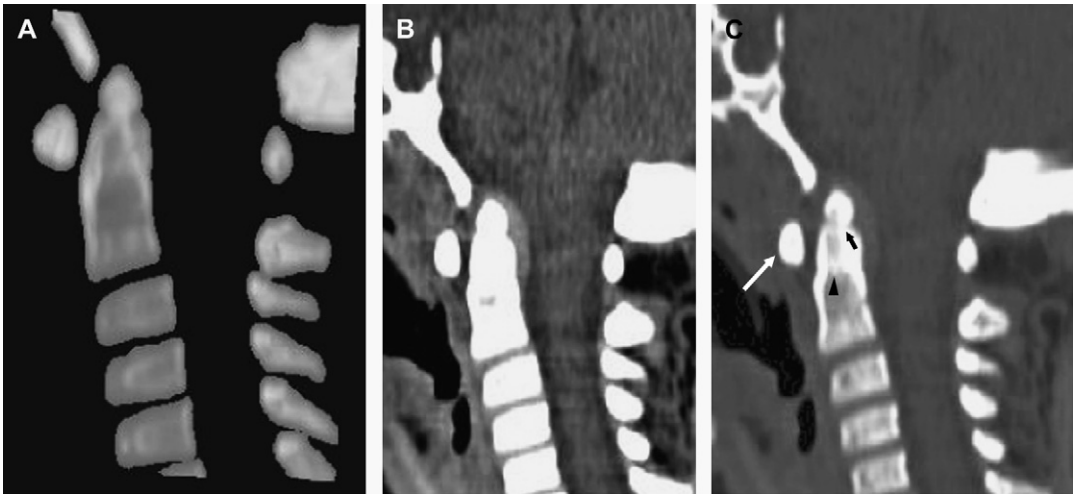

Fig. 14. CT of a 4-year-old cervical spine (sagittal views). (*A*) SSD bone settings. (*B*) MPR soft tissue settings. (*C*) Bone settings with body of C1 (*white arrow*), ossification of subdental synchondrosis (*arrowhead*), ossification of os terminale, and partial fusion with body of odontoid process of C2 (*black arrow*).

determine any compression or extension into the spinal canal. However, MRI's greatest role is in the evaluation of abnormalities affecting the soft tissues of the pediatric spine [7–10,18,22–24].

MRI is highly dependent on various factors that affect resolution (signal-to-noise ratio). These factors include the field strength of the MRI scanner and which technical parameters to use on the MR scanners, and the problems of physiologic and voluntary patient motion. Spin-echo T1- and gradient echo (GE) T2-weighted (W) or fast spin-echo (FSE) T2-W acquisitions are routinely used to evaluate the pediatric spine (Fig. 15). FSE T2-W pulse sequences scan times are shorter, and the resolution of the bone detail is better, than GE T2-W sequences. However, FSE T2-W pulse sequences do not suppress cerebrospinal fluid motion as well as GE T2-W sequences, and flow (motion) artifacts are more pronounced on the images of the spinal canal in infants and young children and may obscure intraspinal pathology. Therefore, flow compensation parameters should be used. The FSE T2-W pulse sequences do not effectively suppress fat, so if fat suppression is desired, a GE or FSE (with fat suppression) T2-W pulse sequence should be used [7–9,18,23–26].

It is important to obtain at least two MRI projections of the spine in children. The sagittal and axial projections are the most commonly obtained. However, in some children with severe scoliosis, some forms of spinal dysraphism, or paravertebral masses with spinal canal extension, the coronal projection may also have to be obtained.

Prenatal development of the spine

The development of the vertebral column occurs in three stages: membranous, cartilaginous, and osseous (Fig. 16 and 17). The notochord acts as a framework for the developing spine. Lack of development, or an arrest in the development, of the vertebra during the stages of chondrification or ossification can result in various anomalies in the pediatric spine. These anomalies range from sagittal and coronal clefting to an absent or hypoplastic body (Fig. 18) [1,6,10,27,28]. The prenatal development of the spine is discussed in detail in an article elsewhere in this issue.

Postnatal development of the spine

The spine continues to grow and develop postnatally, with major changes occurring in the curvature, vertebrae, ossification process, spinal canal, discs, ligaments, and bone marrow. These

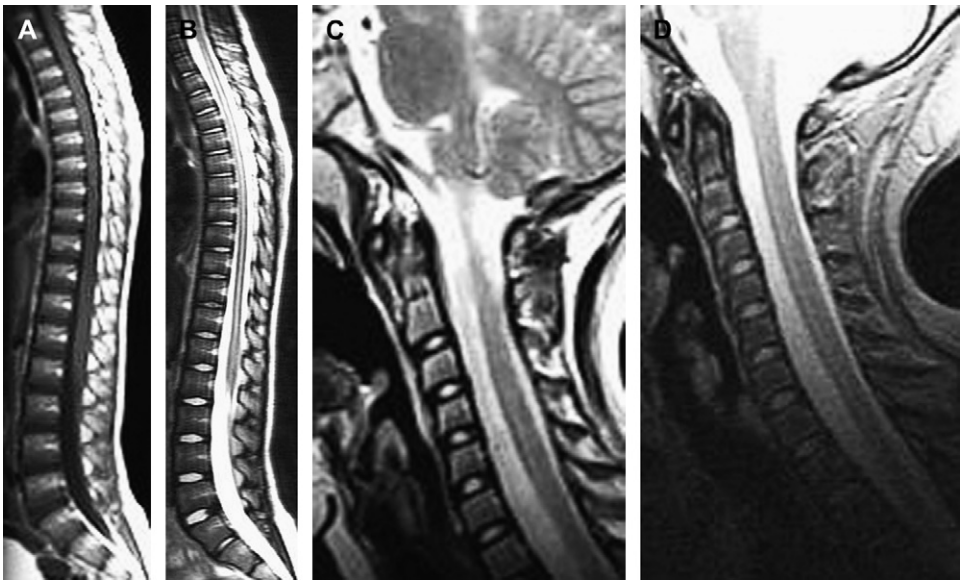

Fig. 15. MRI sagittal T1-W (*A*) and FSE T2-W (*B*) of thoracolumbosacral spine in a 7-year–old child. FSE T2-W (*C*) and GE T2-W (*D*) of cervical spine in an 11-year-old.

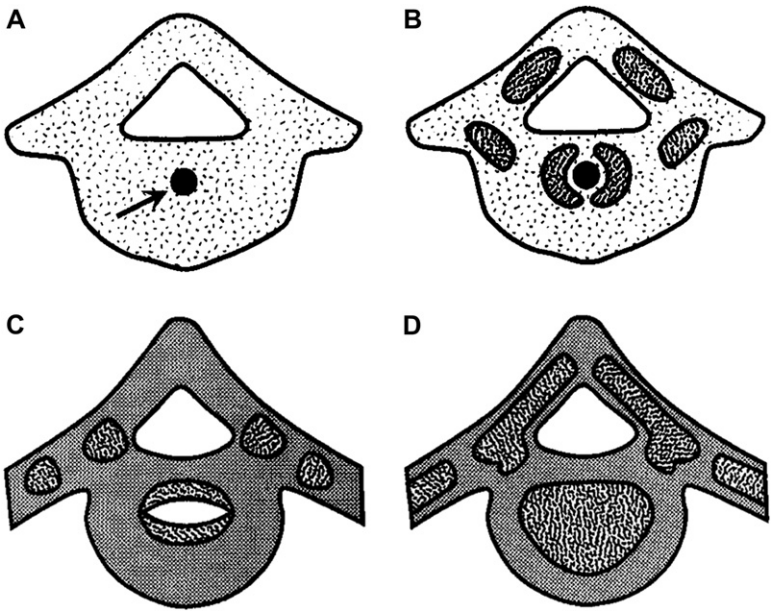

Fig. 16. Axial/transverse images of a thoracic vertebra demonstrating the three stages of development of the vertebral column: (*A*) membranous with notochord (*arrow*); (*B*) cartilaginous with chondrification centers; and (*C*) osseous with ossification centers. (*D*) The appearance of the vertebra at birth, with areas of ossification (centers) seen at birth on the imaging studies. (*From* McLone DG. Pediatric neurosurgery. 4th edition. Philadelphia: Saunders; 2001. p. 123; with permission.)

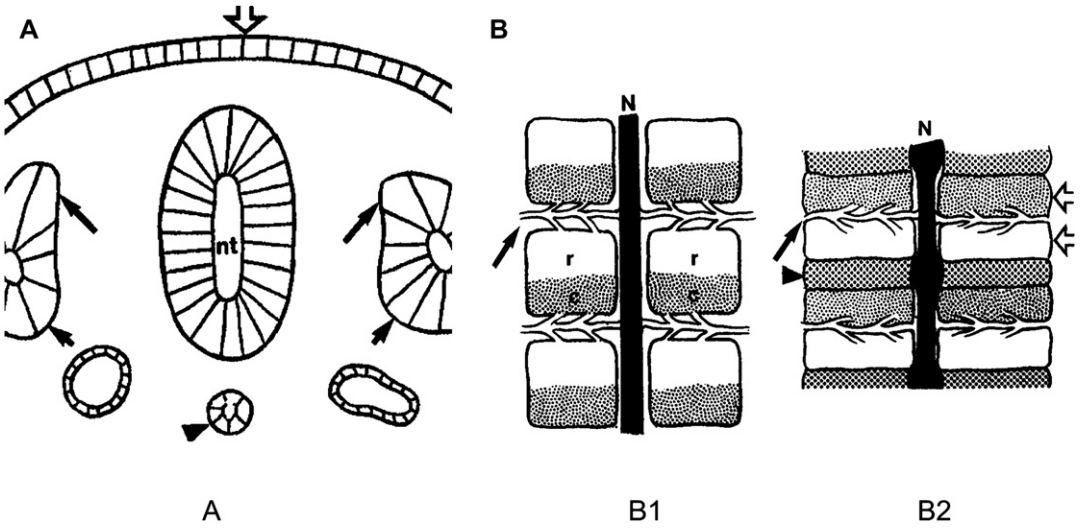

Fig. 17. (*A*) Differentiation of somites into sclerotomes anteriorly (*large arrows*) and demomyotomes posteriorly (*small arrows*) flanked by the neural tube (*nt*) and notochord (*arrowhead*), with all structures surrounded by ectoderm (*large open arrow*). (*B*) Development of sclerotomes into the vertebral column with division of sclerotomes into rostral (*r*) and caudal (*c*) halves (*B1*) and formation of vertebral bodies (*open arrows*) from the fusion of the caudal half of one sclerotome and the rostral half of the adjacent sclerotome; the IVD (*arrowhead*) forms from the caudal half of the somite (*B2*). (*From* McLone DG. Pediatric neurosurgery. 4th edition. Philadelphia: Saunders; 2001. p. 112–4; with permission.)

changes can be seen on the various imaging modalities used to evaluate the pediatric spine [1–6,29–40].

Curvature

At birth, the neonate has a very mild posterior convex curve seen on the lateral view. This gentle kyphosis is the primary curvature of the spine and is seen over its entire length. A totally straight spine is abnormal, even in the newborn. At 3 months, with development of head control, a secondary convex anterior cervical curve develops. This development is the beginning of the normal lordosis of the cervical spine. At 12 months, when the infant begins to crawl and walk, another secondary anterior convex curve develops in the lumbar spine. This development is the beginning of the normal lordosis of the lumbar spine. As the child continues to grow, movement is improved and the paraspinal muscles, ligaments, vertebrae, and discs develop further. The spinal curvature continues to develop into its adult configuration, with its primary curves of kyphosis at the thoracic and sacrococcygeal levels and secondary curves of lordosis at the cervical and lumbar levels (Fig. 19) [1–6].

Vertebrae

The shape of the vertebral bodies in the neonate is usually oval with slightly rounded anterior margins. This shape extends throughout the entire spine, although occasionally it may be more prominent at the lumbar level and the thoracic level may have a slightly squared appearance. The height of a vertebral body is about equal to, or slightly smaller than, the height of the IVD space as seen on lateral CPSI. This simulation of a smaller-sized vertebral body in the neonate is not a true finding. On the CPSI, only the ossified portion of the vertebral bodies is visualized, and the body and the IVD are not visualized, simulating a disc larger than it actually is. Two central indentations or clefts exist within the anterior and posterior walls of the midportion

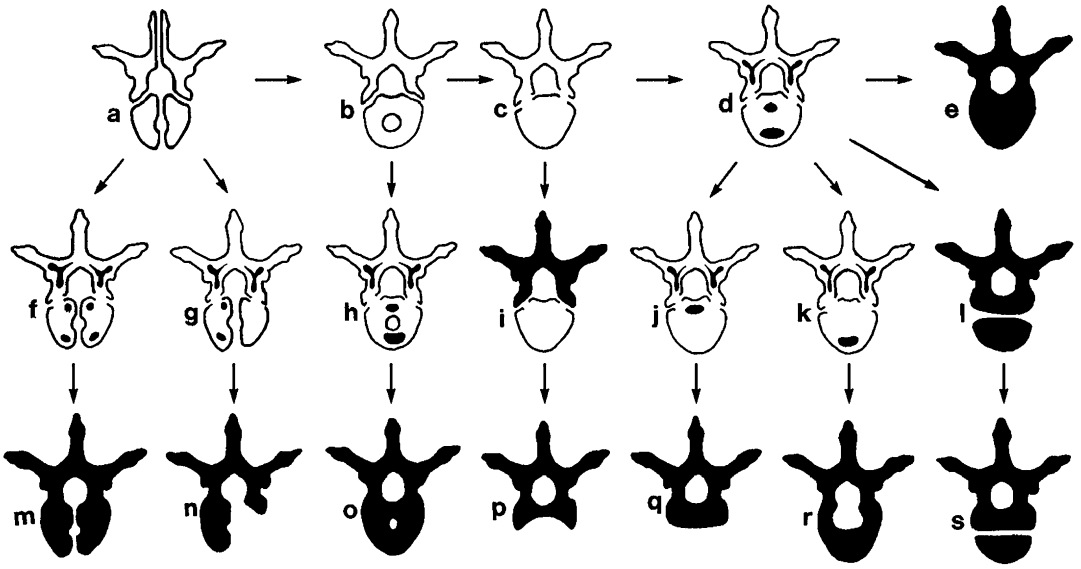

Fig. 18. Axial view of the normal and abnormal development of the vertebrae, with osseous formation in black and cartilaginous formation in white. (*a–e*) Normal formation of a vertebra. (*f–l*) Abnormal formation. (*m–s*) End-stage abnormality. The abnormalities are (*m*) vertebral body sagittal cleft due to nonfusion of the cartilaginous centers, (*n*) hemivertebra due to nonfusion of the cartilaginous centers with unilateral nondevelopment of an ossification center, (*o*) remnant of a notochord, (*p*) agenesis of a vertebral body due to nondevelopment of the ossification centers, (*q*) anterior hypoplasia of a vertebral body due to nondevelopment of the anterior ossification center, (*r*) posterior hypoplasia of a vertebral body due to nondevelopment of the posterior ossification center, and (*s*) vertebral body coronal cleft due to failure of the anterior and posterior ossification centers. (*Modified from* Harwood-Nash DC, Fitz CR. Neuroradiology in infants and children. St. Louis (MO): CV Mosby; 1976. p. 1055; with permission.)

of the vertebral bodies. These anterior and posterior indentations represent vascular channels. The anterior channel consists of nutrient artery and a sinusoidal channel that disappears by the end of the first year of life. However, the anterior channel may be sharply visible up to 3 to 6 years of age and may persist as a slitlike channel with sclerotic margins. The posterior channel consists of a draining vein (the basivertebral vein) and a nutrient artery. The posterior channel does not disappear but persists throughout childhood into adulthood (see Figs. 13, 19) [1–6,29,31,32,34–36].

In the neonate, a normal variation in appearance of the vertebral body of "bone within bone" can be seen on CPSI. This appearance of a lucent area within the outer aspect of the ossified vertebral body is more common in premature infants but can be seen in some series in as many as 50% of full-term normal infants. This appearance is related to the normal ossification process of the vertebral body. It is primarily seen before 6 weeks of age and disappears by 2 to 3 months of age (see Fig. 19) [6,40,41].

The coronal cleft in the vertebral body can be a normal variation or a pathologic process. The coronal cleft is an incidental finding that usually involves the lower lumbar vertebrae (L3-L5), with L4 being the most common. It can be seen occasionally at the thoracic level. It is usually single (38%) but it can involve two (18%), three (18%), or multiple (25%) vertebral bodies. It is seen on the lateral CPSI in the midhalf of the vertebral body. The coronal cleft is seen within the first few months of life and disappears by age 6 to 12 months, although it can persist for up to 2 to 3 years. The cleft is believed to be a result of slow or delayed fusion of the anterior and posterior ossification centers of the vertebral body. Persistence of a coronal cleft is not necessarily significant, although persistent coronal clefts are associated with other segmentation anomalies of the vertebral bodies and spinal dysraphic conditions [1–6].

On the lateral CPSI, the ossified vertebral body does not appear connected to the ossified neural arch (see Fig. 19; Fig. 20). The lucent area at this junction on the lateral CPSI is nonossified neurocentral synchondrosis. The neurocentral synchondroses are paired and connect both sides of the neural arch to the vertebral body. The paired

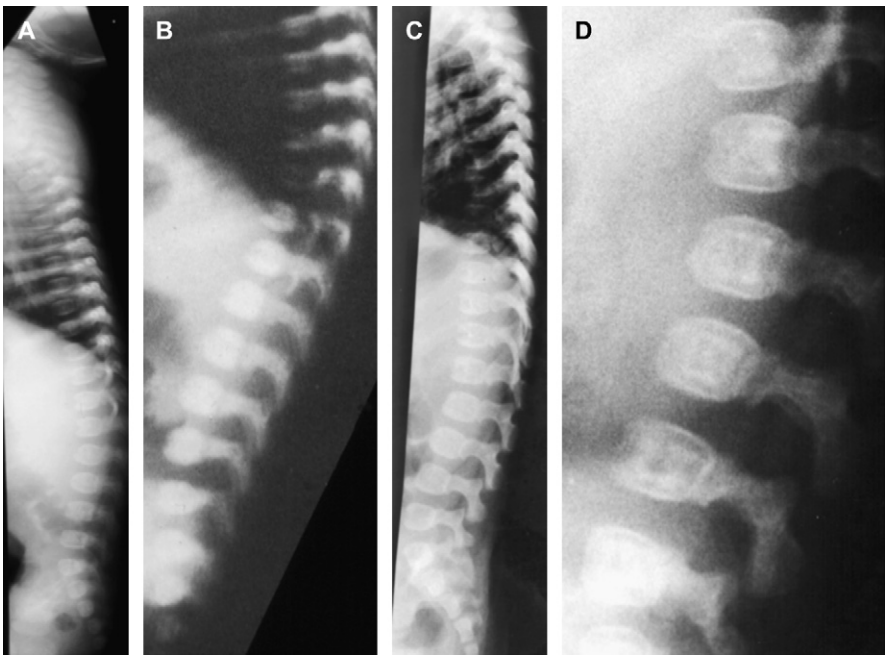

Fig. 19. Lateral CPSI normal spines. (*A*) Relatively straight thoracolumbosacreal spine of a newborn. (*B*) Relatively straight lower thoracic lumbosacreal spine of a 1-month-old with anterior notches for vessels and neurocentral synchondrosis. (*C*) Thoracolumbosacral spine of a 1-year-old with beginning of formation of curvatures. (*D*) Thoracolumbar spine in 5-week-old demonstrating "bone with bone" appearance and anterior notch in vertebral body for anterior vascular channel.

neurocentral synchondroses are seen on AP CPSI along the lateral aspect of each side of the spine. The primary ossification centers of the posterior elements of the vertebrae are present, although the laminae are not fused [1–6,37].

Ossification is present within parts of all of the vertebrae from C1 to sacrum and can be seen on CPSI at birth. C1 and C2 ossify slightly differently than the other vertebrae, and certain important parts (such as the body of C1 and part of the odontoid process) are not seen on the CPSI at birth. The coccyx is not ossified at birth and is not demonstrated on CPSI [38,39].

With further development of the vertebrae at age 2 to 3, the vertebral bodies assume a more rectangular shape, which continues throughout life. The AP diameter of the vertebral body is greater than its vertical height, and its vertical height is greater than the IVD height. The vertebrae continue to ossify, with an increase in density (ossification) occurring within the neurocentral synchondroses by age 3 to 6 [1–6].

By age 5 to 8, superior and inferior steplike recesses appear on the anterior surface of the vertebral bodies, producing an anterior beaking on lateral CPSI (Fig. 21). This finding is caused by an annular rim of cartilage that develops at this time called the ring apophyses. This rim forms over the superior and inferior surfaces of the vertebral bodies. It extends more into the upper and lower anterior borders of the body. This cartilage rim develops outside of the cartilaginous end plates and does not take part in the growth of the vertebral body. This annular ring apophysis begins to ossify and small calcific foci are usually seen at the superior and inferior anterior borders of the vertebral body, most often at the lumbar and thoracic levels and less commonly at the cervical level (Fig. 22). The calcification of the ring apophysis begins to coalesce and ossify to form a complete ring by puberty and to fuse with the remainder of the vertebral body by age 18 to 25. The beaking of the vertebral bodies disappears by puberty (age 10 to 13) but the calcification and later ossification at the superior and inferior rims may persist until 18 to 25 years of age. This normal beaking of the vertebral bodies is never as severe as seen in pathologic conditions such as Morquio's syndrome [1–6].

The last important process that changes the shape and size of the vertebrae is the development of the secondary ossification centers. These centers occur at the tips of the transverse processes, superior and inferior articulating facets, spinous process, and ring apophysis by puberty, with complete ossification by age 18 to 25. These secondary ossification centers can be seen as small lucent areas just proximal to the tips of these processes on CPSI (Fig. 23) (Table 1) [1–6].

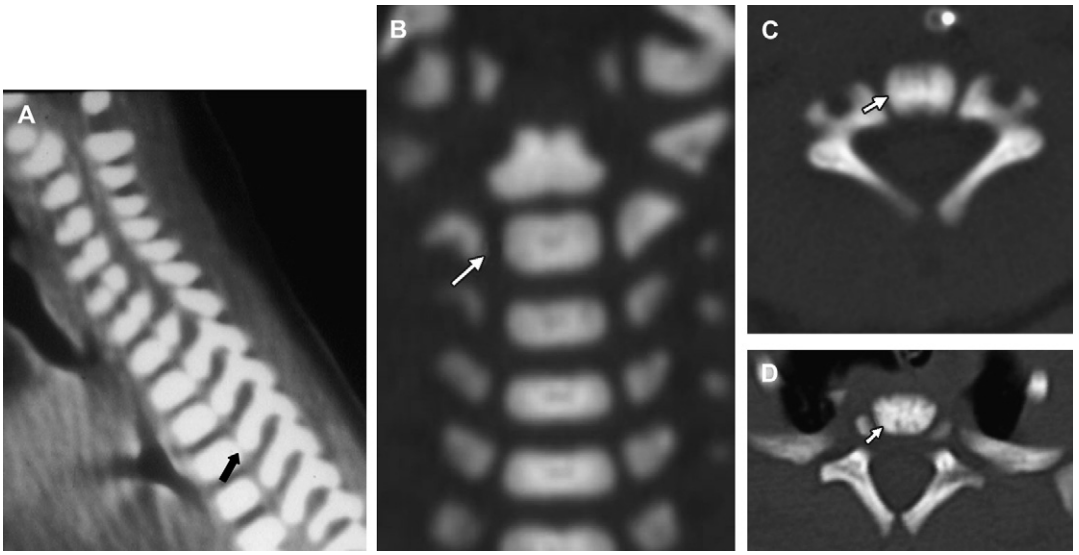

Fig. 20. Neonate's CT scan of spine with nonfused, nonossified neurocentral synchondrosis at junction of lateral masses with the bodies of the vertebrae (*arrows*). (*A*) MPR sagittal off-midline, slightly rotated cervicothoracic spine. (*B*) MPR coronal. (*C*) Axial of C4. (*D*) Axial of T1.

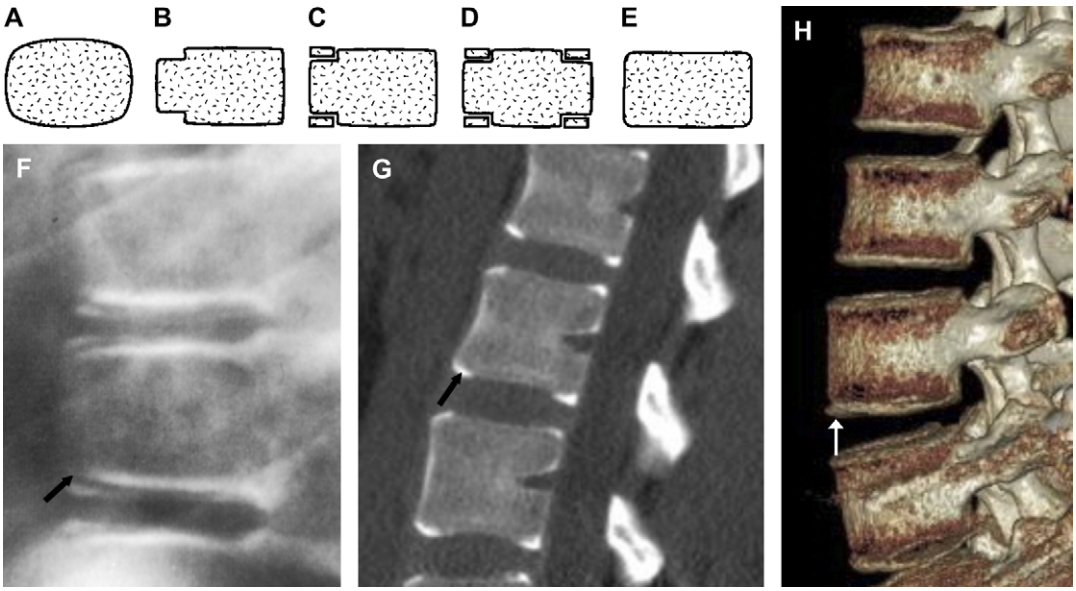

Fig. 21. (*A–E*) Lateral views of the postnatal development of the vertebral body. (*A*) Newborn with oval shape. (*From* McLone DG. Pediatric neurosurgery. 4th edition. Philadelphia: Saunders; 2001. p. 129; with permission.) (*B*) Age 5 to 8, with the beginning of development of the ring apophyses (with superior and inferior steplike indentations). (*C*) Beginning of calcification of the ring apophyses. (*D*) Vertebra with calcification in the anterior and posterior ring apophyses. (*E*) Ossified ring apophyses with a rectangular-shaped vertebral body in a teenager. (*F*) CPSI lateral view of upper lumbar vertebrae, (*G*) CT MPR sagittal of upper lumbar vertebrae, and (*H*) 3D VRT lateral view of lumbar vertebrae, with ossification of portions of the ring apophyses (*arrows*).

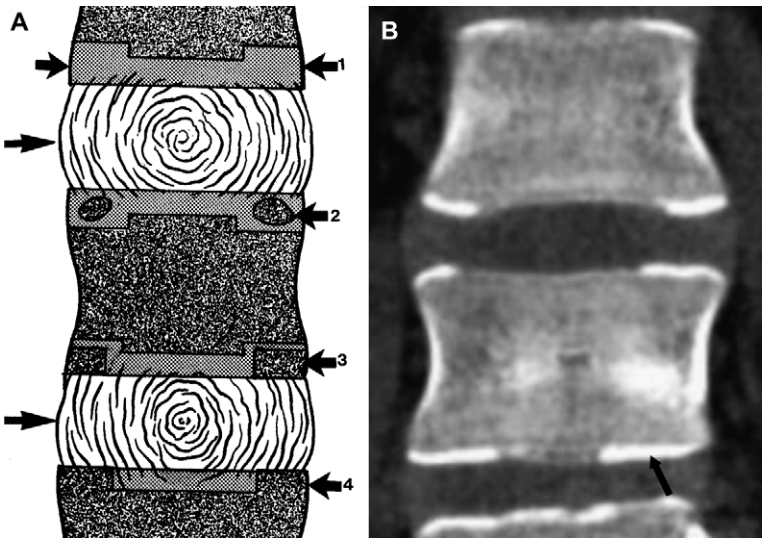

Fig. 22. (*A*) Sagittal view of the lumbar spine showing the relationship of IVDs (*large arrows*) to ossification of the ring apophysis with cartilaginous ring (*1*), appearance of ossification centers (*2*), further enlargement of ossification centers (*3*), and fusion of ossification of the ring to the vertebral body (*4*). (*Modified from* Silverman FN, Kuhn JP. Caffey's pediatric x-ray diagnosis: an integrated imaging approach. St. Louis (MO): CV Mosby; 1993. p. 134; with permission.) (*B*) CT MPR coronal view of upper lumbar spine with ossification in ring apophysis area of increased density (*arrow*). (*From* McLone DG. Pediatric neurosurgery. 4th edition. Philadelphia: Saunders; 2001. p. 112–4; with permission.)

Table 1
Maturation of the spine

Vertebrae	Primary ossification centers	Age at presentation	Age at closure	
			Neurocentral synchondrosis	Laminae
C3-L5	1 middle (body)	At birth	3–6 y	1–3 y
	2 lateral (1 in each half of neural arch)	At birth		
C1	Middle (body)	20% at birth; 80% 6–12 mo	5–7 y (average 6 y)	3–4 y
C2	1 body of C2	At birth	3–6 y	3–6 y
	2 lateral (1 in each half of neural arch)	At birth		
	1 body of dens (rarely, 2)	At birth		
	1 tip of dens (os terminale)	2–6 y fuses with body of dens (10–12 y)		

Vertebrae	Secondary ossification centers	Age at presentation	Ossification completed
C3-L5	Superior articulating facets	Puberty (10–13 y)	18–25 y
	Inferior articulating facets	10–13 y	18–25 y
	Transverses processes	10–13 y	18–25 y
	Spinous process	10–13 y	18–25 y
C3-L5	Ring apophyses	Puberty (10–13 y)	18–25 y

From McLone DG. Pediatric neurosurgery. 4th edition. Philadelphia: Saunders; 2001. p. 125; with permission.

Ossification process

The ossification process within the vertebrae is an ongoing process from fetal development until early adulthood. Most primary ossification centers develop with the vertebral bodies and neural arches during the ossification stage of development of the bony spine, beginning at the eighth week of gestation. At birth, these primary ossification centers can be seen as three bony centers within each vertebra from C3 to L5. Each of these vertebrae has one center in the centrum (the vertebral body) and one in each half of the neural arch (Fig. 24). These ossification centers can be seen at birth as areas of increased density (ossification) within the vertebral body and neural arch. Cartilaginous attachments called

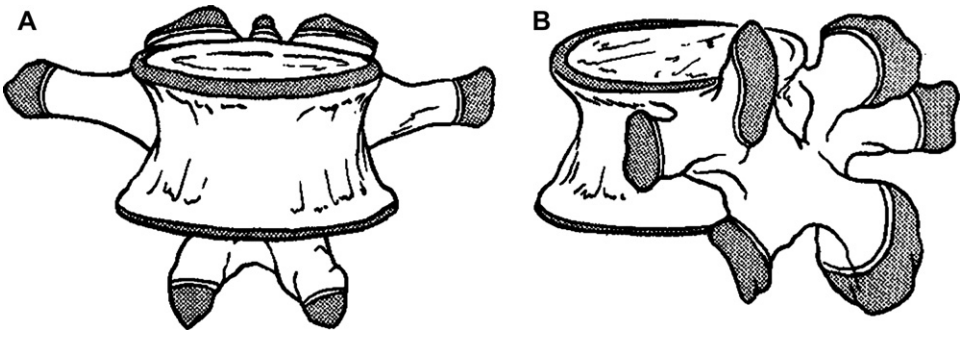

Fig. 23. Vertebra. Anteroposterior (*A*) and oblique lateral (*B*) views of development of secondary ossification centers at the tips of the superior and inferior articulating facets, transverse processes, spinous process, and ring apophysis at the superior and inferior surfaces of the vertebral body. (*From* McLone DG. Pediatric neurosurgery. 4th edition. Philadelphia: Saunders; 2001. p. 129; with permission.)

neurocentral synchondroses are on each side of the neural arch to the vertebral body. These synchondroses appear lucent on CPSI but they ossify and become dense on CPSI by age 3 to 6. This ossification proceeds in an orderly fashion from cephalad to caudal, with ossification occurring first in the cervical vertebrae at age 2 to 3 and progressing inferiorly, with completion by age 6 to 7 in the lumbar region. When the ossification process is complete in the neurocentral synchondroses, the vertebral body is fused to the neural arch. The laminae fuse posteriorly in the midline by age 1 to 3. This process continues in an orderly fashion from inferior to superior, with the laminae fusing in the lumbar area beginning at the end of the first year of life and progressing superiorly, with fusion of the cervical laminae by 3 years of age (Fig. 25) [1–6].

The primary ossification centers of C1, C2, sacrum, and coccyx appear at slightly different times when compared with the rest of the vertebrae (C3-L5). The atlas (C1) commonly has two primary ossification centers at birth, one in each half of the neural arch. The primary ossification center in the body of C1 is only present 20% of the time at birth. It usually appears between the sixth to the twelfth month of life. The neurocentral synchondroses of C1 usually fuse by age 5 to 7 (about 6) and the laminae fuse by age 3 to 4, although nonfusion of the laminae is a common malformation seen at C1 (Figs. 26 and 27) [1–6,38,42].

The axis (C2) has four primary ossification centers at birth, one within the half of each neural arch, one in the body of C2, and one in the body of the dens of C2. The body of the dens (odontoid process) initially has two ossification centers (one on each side) during fetal development. These two ossification centers usually fuse before birth, with one center appearing at birth on CPSI. At times, the two ossification centers may not fuse until 3 months, or up to 1 to 2 years after birth. When this occurs, the odontoid process (body of the dens) has a bifid appearance on AP CPSI. The primary ossification center at the tip of the dens, called the os terminale, usually does not develop until age 5 to 6, although it may be seen as early as the first or second year of life. It appears as a small triangle or round area of density at the tip of the dens (atop the body of the dens). The os terminale fuses with the body of the dens by age 10 to 12, although, rarely, it may not fuse and may persist as a small ossicle. The body of the dens joins the body of C2 at the subdental synchondrosis, which appears as a lucent line slightly below the plane of the superior border of the body of C2. This line disappears (ossifies) by age 4 to 6, although it may persist as a small lucent line up to age 10. Complete ossification of the subdental synchondrosis fuses the body of the dens to the body of C2. The neurocentral synchondroses of C2 ossify by age 3 to 6 and the laminae fuse posteriorly by age 3 to 4 (Figs. 28 and 29) [1–6,39,42].

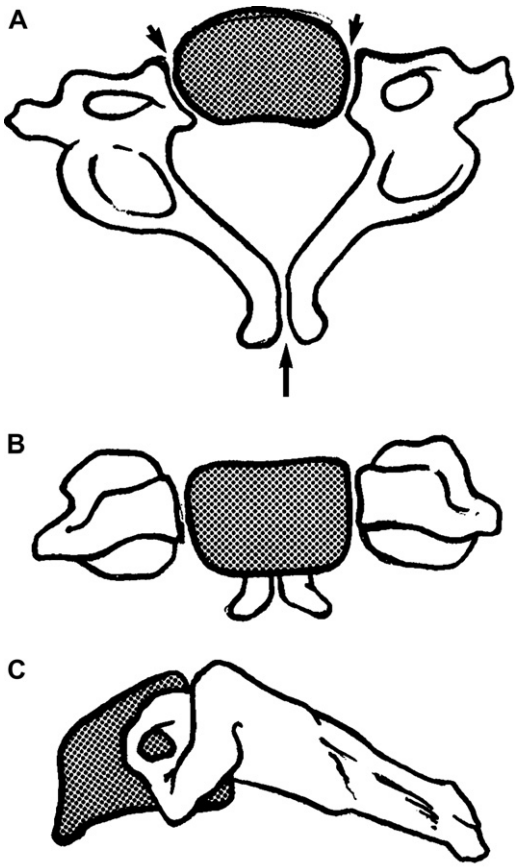

Fig. 24. (*A–C*) Vertebra from C3-7, which is representative of the vertebra from C3-L5, demonstrating the three ossification centers for the body and each of the neural arches. The neurocentral synchondroses (*small arrows*) and ununited laminae (*large arrow*) are present. (*From* Malone DG. Pediatric neurosurgery. 4th edition. Philadelphia: Saunders; 2001. p. 130; with permission.)

An ossification center is seen in each of the bodies of the sacrum at birth and within each side of the neural arch (see Fig. 19A, C). Ossification may vary and may not be complete in the sacrum until age 18 to 20. During infancy, the sacral vertebrae are separated from each other by intervertebral fibrocartilage. The two lower vertebrae fuse around the 18th year of life, and fusion proceeds gradually

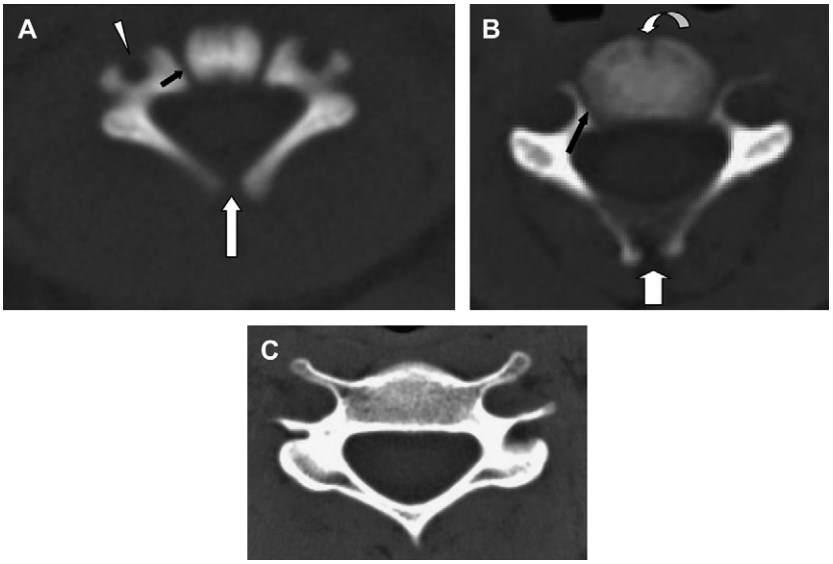

Fig. 25. CT axial (bone settings) of representative cervical vertebrae of C3-7. (*A*) A 3-day-old child with ossification in the body (centrum) and each half of the neural arch, with neurocentral synchondrosis (*black arrow*), transverse foramina (*white arrowhead*), and ununited laminae (*large white arrow*). (*B*) A 4-day-old child with incomplete ossification of the neurocentral synchondrosis (*small arrow*) and laminae (*large arrow*), and persistent anterior channel (*curved arrow*). (*C*) A 16-year-old with complete ossification of vertebra. (*From* McLone DG. Pediatric neurosurgery. 4th edition. Philadelphia: Saunders; 2001. p. 112–4; with permission.)

in a cranial direction until the entire sacrum is united. The vertebral arches unite with the bodies of the lower sacral vertebrae at approximately age 2, and the upper segments unite at approximately age 6. This development occurs by fusion (ossification) of the neurocentral synchondrosis.

The coccyx is not ossified at birth. Each coccygeal segment ossifies from a single center. The ossification center for the first coccygeal vertebra appears approximately at age 4, the second between ages 5 and 10, the third between ages 10 and 15, and the fourth between ages 14 and 20. At times, the segments may undergo bony fusion, but generally, they are united with one another by fibrocartilage.

Secondary ossification centers appear in the vertebrae from C3 to L5 at around puberty (age 10 to 13) and completely ossify by age 18 to 25. These secondary ossification centers appear at the tips of the transverse processes, superior and inferior articulating processes, spinous process, and ring apophyses [1–6].

Simple spina bifida, ununited laminae posteriorly at one or two spinal levels, can occur without any significance or it can be associated with certain forms of spinal dysraphism, especially if multiple segments are involved. Simple spina bifida can be seen in 9% to 22% of children and 1% to 9% of adults in certain series based on CPSI. The overall occurrence of simple spina bifida is seen more commonly at L5-S1, C1, C7-T1, and the lower thoracic level, in decreasing order of frequency. Transitional vertebrae exist in the vertebral column at the cervicothoracic, thoracolumbar, and lumbosacral levels. Variations that are not malformations, including those involving the cervical ribs, hypoplastic or absent twelfth ribs, lumbarization of the first sacral segment or first lumbar ribs, and sacralization of the fifth lumbar segment, occur at these levels [6,42].

Other anatomic variations consist of occipitalization of the C1 vertebral body, third condyle (spur attached to the inferior edge of the anterior border of the foramen magnum); absence of the posterior arch of C1 (usually a fibrous ring is seen); anterior cleft in the anterior ring of C1, secondary to failure of the central ossification center to develop; bifurcation or duplication of the odontoid, os terminale; absence of pedicles: and thinning of pedicles at the thoracolumbar junction (commonly T11-L2) [6,42].

Pseudosubluxations

During the postnatal maturation of the spine, certain spine measurements and pseudodisplacements in children differ in comparison with adults. The

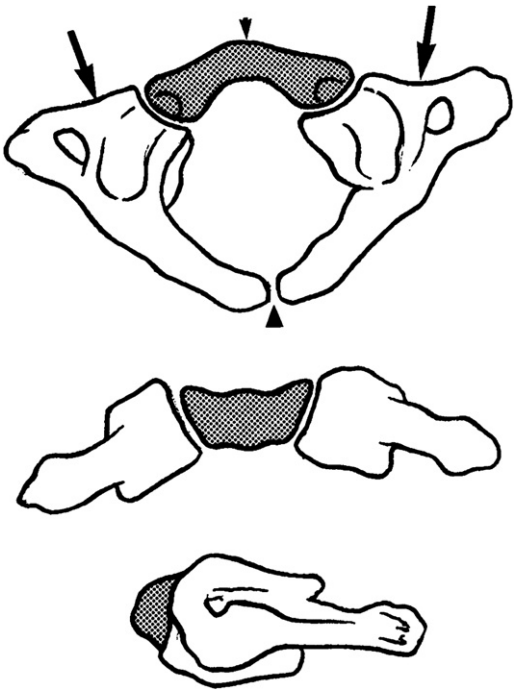

Fig. 26. C1 in an infant with the body of C1 (*small arrow*), lateral masses (*large arrows*), and ununited laminae (*arrowhead*). (*From* McLone DG. Pediatric neurosurgery. 4th edition. Philadelphia: Saunders; 2001. p. 132; with permission.)

atlantoaxial relationship between the posterior margin of the arch of C1 and the anterior margin of the odontoid process (C1-dens) usually measures 2 to 4 mm but may be as great as 5 mm in children or young adults. This distance can normally increase 1 to 2 mm on the flexion lateral view but the overall measurement should not exceed 5 mm. The variance in this distance is felt to be a combination of laxity of surrounding ligaments and incomplete ossification of the dens.

Pseudosubluxations (anterior displacements) of the body of C2 and C3 or C3 onto C4 are 3 to 4 mm but can vary from 1 to 5 mm when the spine is flexed from the neutral position on lateral CPSI. These pseudosubluxations occur during infancy and childhood, up to 10 years of age (usually seen between ages 1 and 7) (see Fig. 11). After age 10, pseudosubluxations can be seen at C4-5 or C5-6. Differentiation of these pseudosubluxations from true subluxations depends on the maintenance of the normal alignment of the spinolaminar line. Normally, the alignment of the posterior arches (spinolaminar junction lines) is maintained in these pseudosubluxations. These

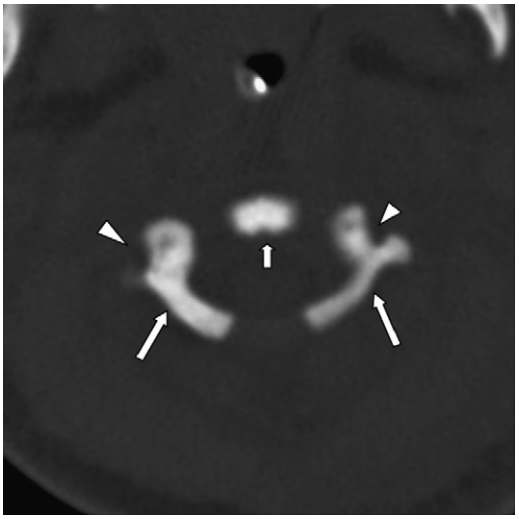

Fig. 27. CT axial (bone settings) image of a 2-day-old neonate with ossification center in each lateral mass of C1 (*large arrows*), transverse foramen (*arrowheads*), and ossification center of odontoid process of C2 (*small arrow*). The ossification center in the body of C1, which lies anterior to odontoid process, is not seen. It is commonly not present on CT or CPSI until the 6th to 12th month of life.

areas of pseudosubluxations occur at the principle cervical motion, which in the infant and young child occurs at the C2-3 or C3-4 level. The principle cervical motion changes to the C4-5 or C5-6 level at approximately 10 years of age [1–6,42–45].

Intervertebral disc

Changes also occur in the maturation of the IVD. The disc is ovoid in appearance on CPSI and blends into the nonossified vertebral end plates in the neonate and infant. With ossification and development of the vertebral bodies, the disc appears rectangular in shape on CPSI by age 2 to 3. However, the true shape of the disc in the neonate is best seen on the T2-W sagittal view as a hyperintense ovoid or rectangular structure separate from the cartilaginous end plates of the vertebral body. It is approximately one third to one fourth the size of the body, depending on the age of the child. The disc is larger in the newborn and infant [1–6,23,33–35,46].

The disc is a vascular structure at birth. It receives its vascularity from the adjacent vertebrae. The arterial supply is primarily from nutrient arteries of the body extending to the

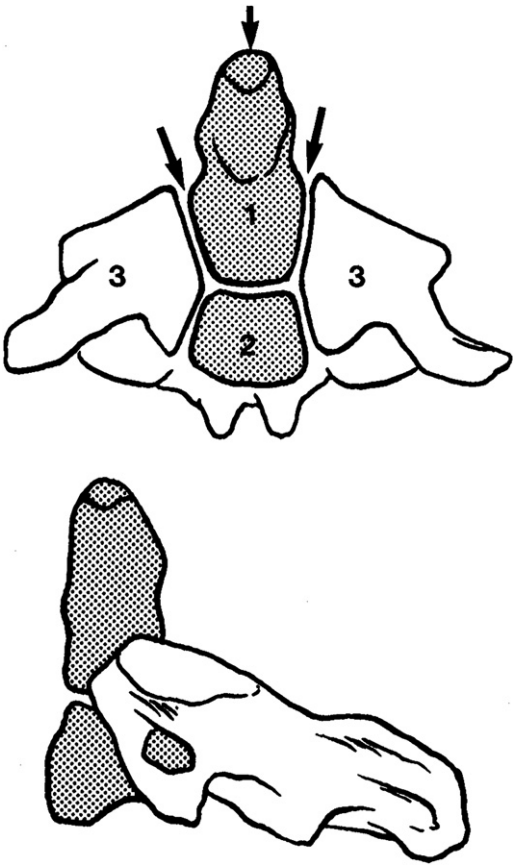

Fig. 28. Ossification centers of C2 with os terminale (at tip of dens) (*small arrow*), body of dens (*1*), body of C2 (*2*), lateral masses (*3*), and neurocentral synchondroses (*large arrows*). (*From* McLone DG. Pediatric neurosurgery. 4th edition. Philadelphia: Saunders; 2001. p. 133; with permission.)

cartilaginous end plates and adjacent discs. This vascularity gradually decreases throughout infancy and early childhood until about age 4, when the disc becomes an avascular structure. The disc is composed of a central nucleus pulposus and an outer ring, the annulus fibrosus. The nucleus pulposus develops from notochordal and perichordal mesenchyme. It consists of a mucoid substance, oncotic proteoglycan (product of notochordal degeneration), water (88% at birth), and a few fibrocartilaginous strands. The annulus fibrosus develops only from perichordal mesenchyme and consists of fibrocartilage and water (78% at birth). As the disc matures through childhood and into early adulthood, it loses water. By age 25 to 30, the water content of the nucleus pulposus has decreased to 76%, and that of the annulus fibrosus to 70%. The normal disc is not visualized on CPSI but it can be seen on CT (see Figs. 1, 5, 12, 13, and 21). It is best imaged on MRI because of its high water content (see Figs. 1, 5, 12, 13 and 22) [1–10,23,27].

The ligamentous attachments of the spine are not seen on CPSI. Some of the ligaments can be demonstrated on the soft tissue settings on CT but they are not well delineated. The ligaments are best seen on MRI on T2-W images. The spine has two types of joints. The IVDs form amphiarthroses and the facets form diarthrodeses joints, which are demonstrated on CT and MRI.

Spinal canal and intervertebral foramina

The bony spine grows by enchondral and membranous ossification. The vertebral body grows in height by enchondral ossification at its cartilaginous end plates and in width by membranous ossification. The posterior elements grow by membranous ossification. At birth, the average length of the spine without the sacrum is 20 cm, during first 2 years of life it is 45 cm, at puberty it is 50 cm, and in the adult it averages 60 to 75 cm. The maximum length is attained at age 22 to 24. The parts of the spine grow at different rates. At birth, the cervical spine is 25%, the thoracic spine is 50%, and the lumbar spine is 25% of the total length of the spine without the sacrococcygeal region. In the adult, the cervical is 17%, the thoracic 50%, and the lumbar 33% of the total length of the spine [4,47].

The spinal canal grows by enchondral and membranous ossification of the vertebrae and by enchondral ossification of the neurocentral synchondroses. The spinal canal grows as the vertebrae grow, but once the neurocentral synchondroses and the midline posterior arch ossify and close, the spinal canal can no longer grow. The spinal canal diameter reaches adult size by age 6 to 8, after which very little diametric canal growth occurs. In the newborn and during infancy, the spinal canal is oval in shape and its transverse diameter is larger than its sagittal diameter. By late childhood, it assumes a more round-to-oval configuration in the cervical, thoracic, and upper lumbar regions, and is round to triangular in the lumbar and sacral regions [1–6].

At birth to age 3 months, the sagittal diameter of the spinal canal is 1.0 cm in the cervical region and 1 to 1.3 cm in the lumbar region. At the end of the first decade of life, the spinal canal should approach adult size, whereby the sagittal diameter

is 15 to 27 mm in the cervical, 17 to 22 in the thoracic, and 15 to 27 mm in the lumbar spine. The transverse diameters are larger than the sagittal diameters. The interpedicular (transverse) measurements of the spinal canal have been used and delineated more succinctly in the literature; Elsberg and Dyke in adults, French and Peyton in infants and children, Simril and Thurston in children, Landdmesser and Heublein in children from 1 to 15, and Hinck, Clark and Hopkins in children and adults [48–57].

Vascularity and vascular structures

The vascularity to the bony spine is provided by arteries and draining venous plexuses and veins. The arterial trunks to the spine are virtually complete by the seventh month of gestation. The cervical region is supplied by arterial vessels from the vertebral, ascending cervical, cervical, and occipital arteries. The thoracic spine receives arteries from the dorsal branches of the intercostal arteries. The lumbar spine is supplied by the posterior branches of the lumbar arteries. These arteries eventually supply the bony spine by nutrient arterial branches. In the newborn, arterial vessels can be seen extending anteriorly into the middle of the vertebral body. The main vessel is a nutrient artery and it forms an anterior channel and anterior notch seen at birth and during infancy in the middle of the vertebral body on CPSI and CT. This anterior channel usually disappears by age 1; however, it may persist and be sharply visible for up to age 3 to 6, or even in older children, as a slitlike notch with sclerotic margins. On MRI, this anterior nutrient artery can be seen on sagittal T1-W images in the neonate and young infant (Fig. 30) [1–10,24,58,59].

The venous drainage of the spine is by way of venous plexuses and veins that drain into vertebral veins. Epidural veins posterior to the posterior border of the vertebral body within the anterior epidural space can be seen as soft tissue densities running as bilateral parallel bundles along the anterolateral aspect of the spinal canal. These bundles are best appreciated in the epidural fat on the axial CT scans filmed with soft tissue settings and as vascular bundles with signal void or mixed signal on axial MRI scans. These venous bundles represent a combination of the retrovertebral plexus of veins and paired anterior internal vertebral veins. The basivertebral vein is part of the venous drainage of the vertebral body. It is at the midpoint of the vertebral body, best seen on axial CT scan as a Y or V lucent structure draining posteriorly into the retrovertebral plexus at the midline, as a single venous channel, or as two channels separated by a bony septum. On the lateral CPSI, sagittal MPR CT, and sagittal T1-W and T2-W MRI, the basivertebral vein can be seen as a posterior channel and notch in the middle of the vertebral body. It is present at birth and persists throughout life. These venous channels will enhance with contrast [1–10,18,23,24].

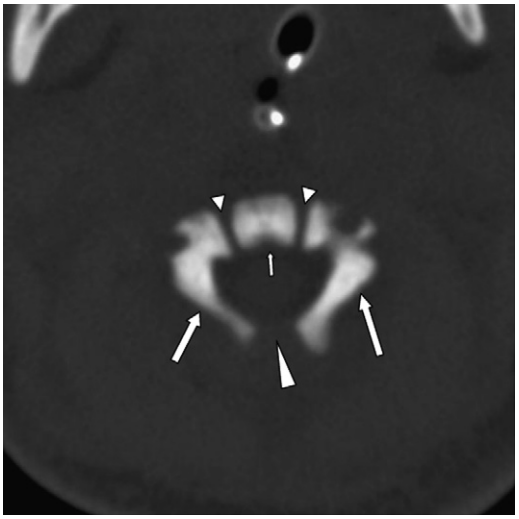

Fig. 29. CT axial (bone settings) image of C2 in a 2-day-old child with ossification in the body (*small arrow*), lateral masses (*large arrows*), neurocentral synchondroses (*small arrowheads*), and ununited laminae (*large arrowhead*).

Bone marrow

The marrow spaces in the spine are predominantly within the vertebral bodies. At birth, the vertebral body consists of cartilaginous end plates, an outer shell of cortical bone, and an inner matrix composed of cancellous (trabeculae) bone and cellular (bone) marrow. Bone marrow is composed of hematopoietic cells, fat cells, and reticulum cells. Marrow can be categorized as red (hematopoietically active) or yellow (hematopoietically inactive). Red marrow is a rich vascular network made up of water (40%), protein (20%), and fat (40%). Yellow marrow consists of a sparse vascular network of water (15%), protein (5%), and fat (80%) [7–10,23,27].

During fetal development, all bone marrow is red. At birth, the marrow is almost totally red. Over the next 10 years, the red marrow begins its progressive conversion to yellow marrow. By age

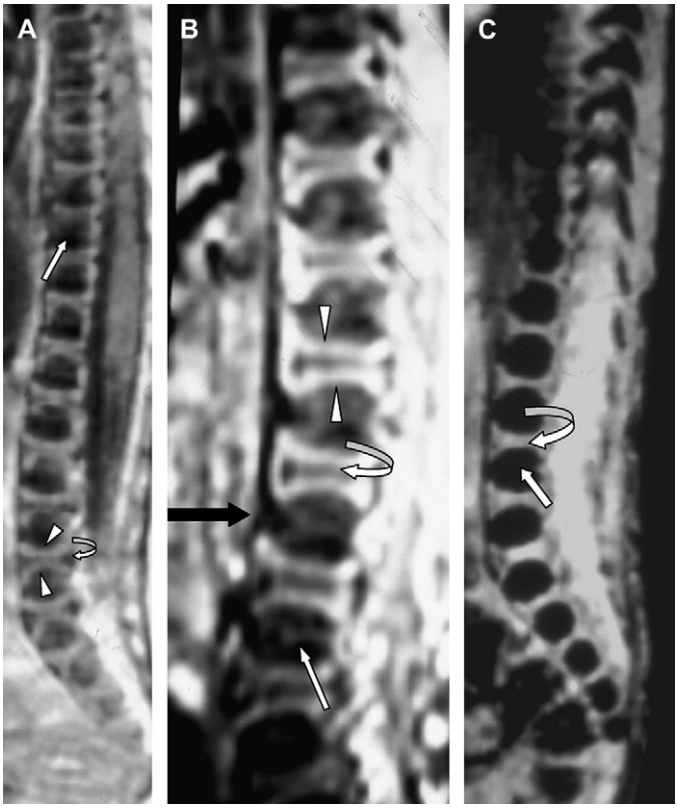

Fig. 30. MRI of newborn spine lower thoracolumbosacral. (*A*) Sagittal T1-W, with marked hypointense vertebral bodies' ossification center (*white arrow*), marked hyperintense cartilaginous end plates (*white arrowheads*), iso/hypointense discs (*curved arrow*). (*B*) Sagittal T1-W of thoracolumbar area with nutrient artery extending into anterior channel of the vertebral bodies (*back arrow*). (*C*) Sagittal GE T2-W of thoracolumbosacral spine with marked hypointense vertebral bodies' ossification center (*arrow*), marked hyperintense cartilaginous end plates, and hyperintense discs (*curved arrow*).

10, only 58% of the bone marrow is red, with 42% being yellow. The conversion to the dominant pattern of yellow marrow (adult pattern) is completed by early adulthood, around age 25. Red marrow is still present, but most of the marrow is yellow. MRI is the best modality to evaluate the changes in bone marrow [7–10,23,27,46,60–63].

MRI of the normal pediatric spine

The MRI appearance of the pediatric spine is related to signal from the vertebrae and IVDs. The signal intensity of the vertebrae is caused by its outer cortical shell and inner matrix of bone marrow. The signal intensity of the disc is primarily from the water content of the nucleus pulposus. The pediatric spine demonstrates changes related to the development of the vertebrae during the first 2 years of life. The changes in the development of the vertebrae are related to the cartilaginous end plates and the ossification centers, consisting of mainly red (hematopoietic) marrow. The vertebral bodies/ossification centers and the cartilaginous end plates are considered one unit. The cartilage is hyaline, which forms the endochondral growth layer around the ossification centers at the end plates. These changes are more pronounced on MRI during the first 24 months of life and more readily demonstrated in the vertebral bodies on the different pulse sequences. The GE T2-W pulse sequence suppresses fat and the red bone marrow appears more hypointense on these images, compared with the FSE T2-W pulse sequence at all ages. Changes also occur with the shape of the vertebral column and the IVDs [7,8,24,46,63]. The MRI signal changes outlined in the following discussion of the postnatal maturation of the spine

are based on a high field strength 1.5 Tesla MRI scanner (Table 2).

From birth to 1 month of life (neonatal period), the spine is relatively straight because weight-bearing forces are inconsequential at this time. The vertebral body (ossification center) is oval in shape and demonstrates marked hypointensity on T1-W, marked hypointensity on GE T2-W, and moderate hypointensity on FSE T2-W images because of the almost totally red marrow content of the ossification center. The cartilaginous end plates are markedly hyperintense on T1-W and GE T2-W images, with mild hyperintensity on T2-W images. The cartilaginous end plates comprise about 25% to 50% of the vertebral body height. The IVD is a thin band that is iso- or hypointense on T1-W images and hyperintense on T2-W images, and is about 20% to 30% of the height of the vertebral body. The posterior elements with their ossification centers follow the same signal as the vertebral bodies. The neural foramina are round (see Fig. 30; Figs. 31 and 32) [24,46,63,64].

By age 1 month to 6 months, the spine is still relatively straight. During this stage, a thin black rim/cortex surrounding the ossification center becomes visible on some of the pulse sequences. The vertebral body (ossification center) is oval in shape and demonstrates the beginning of mild, slight hyperintensity to its superior or inferior aspects, with a larger central area of hypointensity on T1-W and FSE T2-W images and continued hypointensity on the GE T2-W images. The cartilaginous end plates are iso- to moderately hyperintense on T1-W images, iso- to mildly hyperintense on T2-W images, and mild to moderately hyperintense on GE T2-W images, and comprise 20% to 30% of the vertebral body

Table 2
MRI changes in the normal pediatric spine from birth to age 3

Vertebral body	T1-W	GE T2-W	FSE T2-W
Birth to 1 month of age			
Ossification center	Marked hypointensity	Marked hypointensity	Moderate hypointensity
Cartilaginous End plates	Marked Hyperintensity	Marked Hyperintensity	Mild Hyperintensity
Intervertebral disc	Iso- or hypointensity	Hyperintensity	Hyperintensity
1 to 6 months of age			
Ossification center	Slight hyperintensity; superior or inferior aspect with larger central area of hypointensity	Hypointensity	Slight hyperintensity; superior or inferior aspect with larger central area of hypointensity
Cartilaginous End plates	Iso- to moderate Hyperintensity	Mild to moderate Hyperintensity	Iso- to mild Hyperintensity
Intervertebral disc	Iso- or hypointensity	Hyperintensity	Hyperintensity
6 to 12 months of age			
Ossification center	Iso- or slight hyperintensity	Slight hypointensity	Iso- or slight hyperintensity
Cartilaginous End plates	Not well seen Iso- to hypointensity	Not well seen Iso- to hypointensity	Not well seen Iso- to mild hyperintensity
Intervertebral disc	Iso- to hypointensity	Hyperintensity	Hyperintensity
1 to 2 years of age			
Ossification center	Mild to moderate hyperintensity	Slight hypointensity	Iso- to slight hyperintensity
Cartilaginous End plates	Not well seen Hypointensity	Not well seen Hypointensity	Not well seen Hypointensity
Intervertebral disc	Hypointensity	Hyperintensity	Hyperintensity
2 to 3 years of age			
Ossification center	Slight hyperintensity	Slight hypointensity	Slight hyperintensity
Cartilaginous End plates	Not well seen Cortical rim surrounding body	Not well seen Cortical hypointense rim surrounding body	Not well seen Cortical hypointense rim surrounding body
Intervertebral disc	Hypointensity	Hyperintensity	Hyperintensity

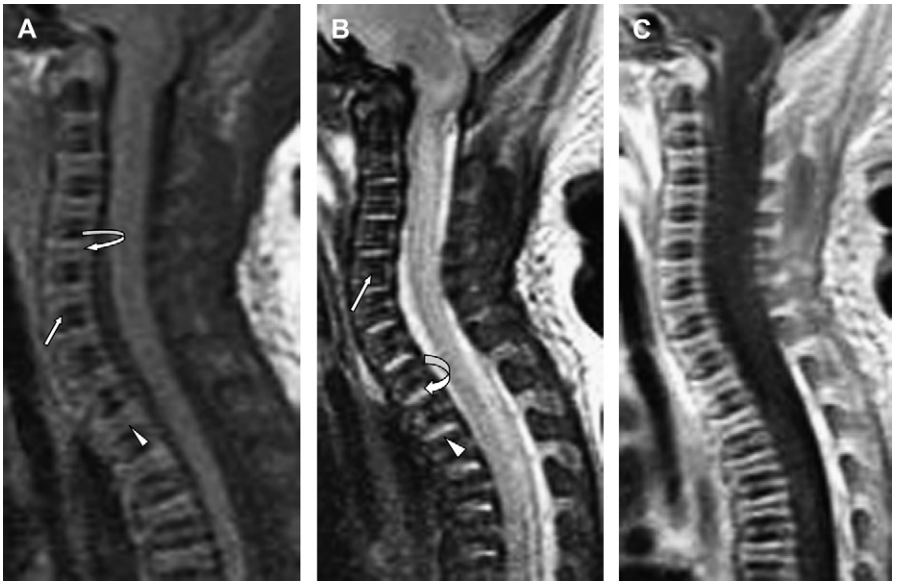

Fig. 31. Cervical spine of newborn sagittal MRI. (*A*) T1-W hypointense vertebral bodies' ossification centers (*white arrow*), hyperintense cartilaginous end plates (*arrowhead*), and isointense discs (*curved arrow*). (*B*) FSE T2-W with hypointense vertebral bodies' ossification centers (*white arrow*), mild hyperintense cartilaginous end plates (*arrowhead*), and isointense discs (*curved arrows*). (*C*) T1-W postgadolinium contrast demonstrating some enhancement of the vertebrae and cartilaginous end plates.

height. During this stage, the signal intensity of the ossification center/vertebral body becomes equal to that of the cartilaginous end plates. The IVD is band shaped, iso- or hypointensive on T1-W images and hyperintense on T2-W images, and 20% to 30% of the height of the vertebral body. The posterior elements follow the same signal as the vertebral body. The neural foramina are round (Fig. 33) [24,46,63,64].

By age 6 to 12 months, the cartilaginous end plates are not as well seen. They blend into the signal of the adjacent disc. The ossification within the cortical rim is more apparent and demonstrates no signal. The cortical rim appears as black on all of the pulse sequences. The spine starts to develop a mild cervical and lumbar lordosis. The normal cervical lordosis develops when the infant begins to have head control. The thoracic kyphosis and lumbar lordosis begin to develop when the child starts to bear weight (crawling and walking). The vertebral body (ossification center) is ovoid to slightly rectangular in shape and demonstrates

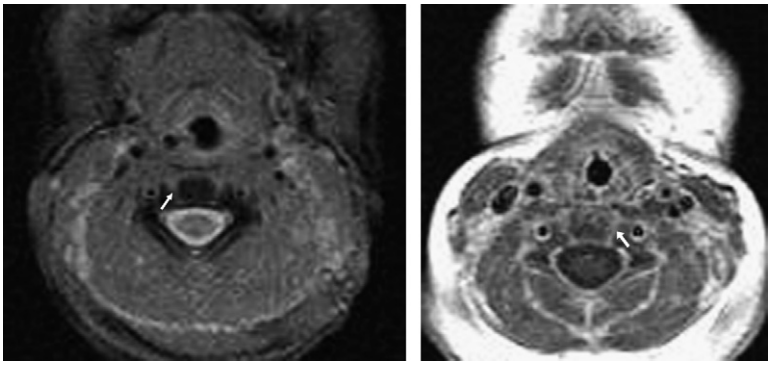

Fig. 32. MRI newborn cervical spine axial images. (*A*) GE T2-W hyperintense neurocentral synchondrosis (*arrow*). (*B*) T1-W postgadolinium contrast image with some enhancement of the neurocentral synchondrosis (*arrow*).

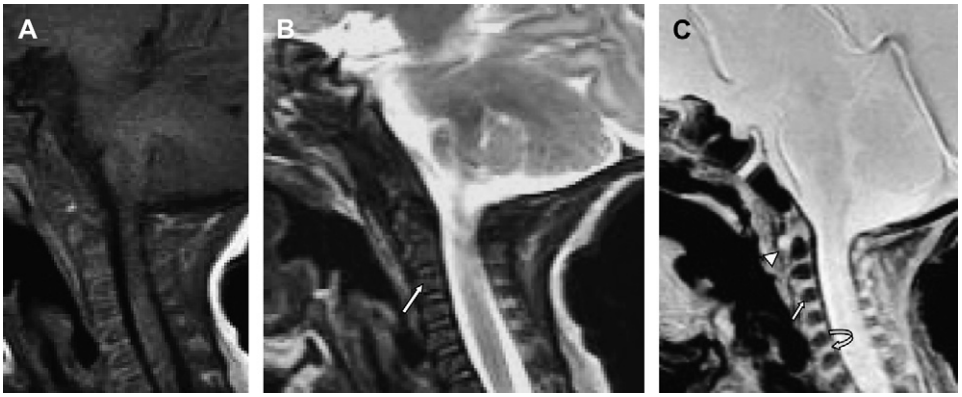

Fig. 33. MRI sagittal of a 3-month-old cervical spine. (*A*) T1-W slight hyperintense peripheral aspect of vertebral bodies' ossification centers with larger central area of hypointensity and a midlinear area of slight hyperintensity related to the basivertebral vein, hyperintense cartilaginous end plates. (*B*) FSE T2 iso- to slight hyperintense ossification centers of the vertebrae (*arrow*). (*C*) GE T2-W hypointense ossification centers (*arrow*), cartilaginous hyperintense body of C1 (*arrowhead*), and hyperintense cartilaginous end plates and discs (*curved arrow*).

Fig. 34. Sagittal MRI of cervical spine in an 11-month-old child. (*A*) T1-W iso- to slightly hyperintense ossification centers of the vertebrae, isointense discs (*curved arrow*), and iso- to hypointense cartilaginous end plates that are not well seen, hypointense cortical rim. (*B*) GE T2-W iso- to slightly hypointense ossification centers, hyperintense discs (*curved arrow*) and iso- to hypointense cartilaginous end plates that are not well seen, hypointense cortical rim.

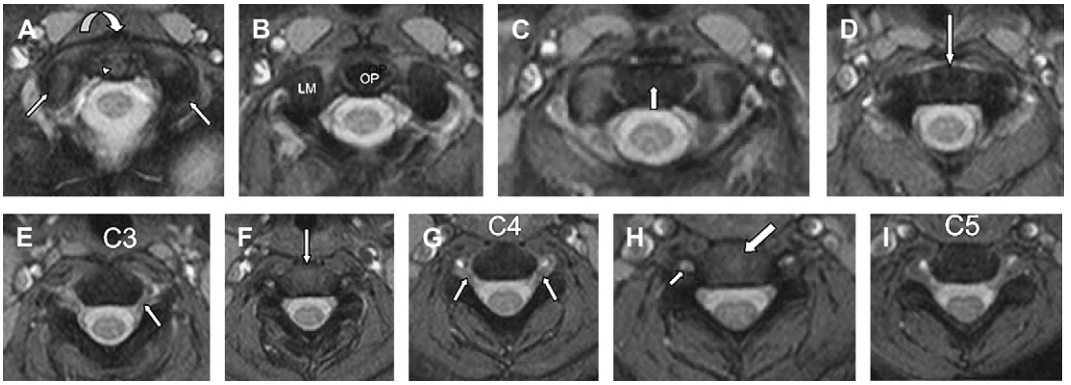

Fig. 35. MRI GE T2-W axial of cervical spine in an 11-month-old child. (*A*) anterior arch (body of C1) (*curved arrow*), cartilaginous tip of the odontoid process (*arrowhead*), superior articulating facets of lateral masses of C1 (*short white arrows*). (*B*) Inferior articulating facets of lateral masses of C1 (*LM*) and odontoid process (*OP*) of C2. (*C*) Junction of odontoid process with body of C2 (*arrow*). (*D*) Body (*arrow*) and lateral masses of C2. (*E*) C3 vertebra with nerve root (*arrow*) in intervertebral foramen. (*F*) C3-4 disc (*arrow*). (*G*) C4 intervertebral neural foramen (*arrows*). (*H*) C4-5 disc (*large arrow*) and transverse foramen (*small arrow*). (*I*) C5 vertebra.

either iso- or slight hyperintensity on T1-W images and FSE T2-W images, or slightly greater superior or inferior areas of mild hyperintensity, with a central area of hypointensity on T1-W images, and slight hyperintensity of the vertebral body on T2-W images. The cartilaginous end plates are not well seen and are mainly iso- to hypointense on T1-W images and iso- to mildly hyperintense on T2-W images, and comprise 20% to 30% of the vertebral body height. The IVD is rectangular shaped, iso- to hypointense on T1-W images, hyperintense on T2-W images, and 20% to 30% of the height of the vertebral body. The posterior elements/spinous processes are iso- to slightly hyperintense on T1- and T2-W images. The neural foramina are round to oval in shape (Figs. 34 and 35) [24,46,63,64].

From 1 to 2 years of age, the spinal curvature has a mild cervical and lumbar lordosis and mild thoracic kyphosis. The vertebral body is more rectangular in shape and demonstrates mild to moderate hyperintensity on T1-W images, iso- to slight hyperintensity on FSE T2-W images, and slight hypointensity on GE T2-W images. By age 2, the cartilaginous end plates and ossification center have reversed their relationship with

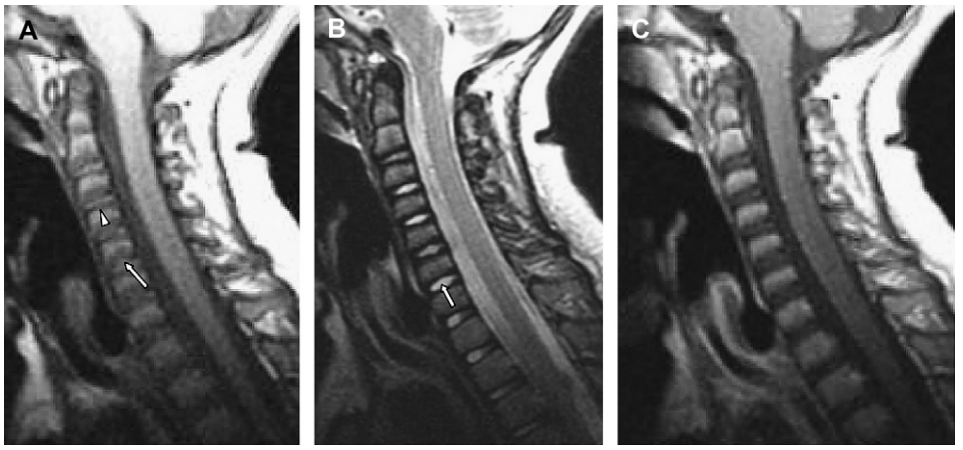

Fig. 36. MRI of cervical spine in 3-year-old sagittal images. (*A*) T1-W slight hyperintensity of vertebrae, isointense discs (*arrow*) and thin cortical hypointense rim (*arrow head*). (*B*) FSE T2-W slight hyperintense vertebrae and more marked hyperintense discs (*arrow*). (*C*) T1-W post gadolinium contrast with no enhancement of the vertebrae.

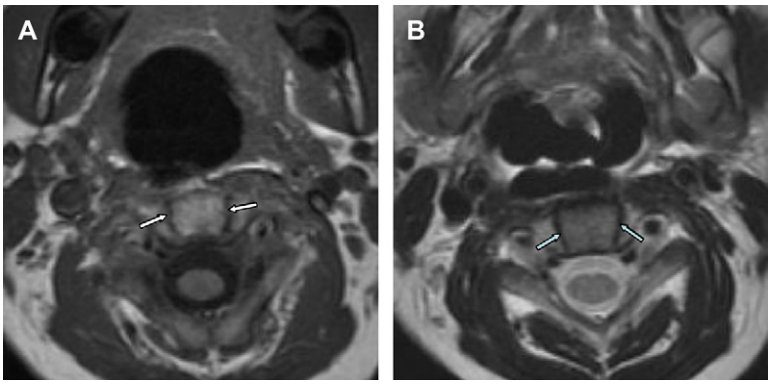

Fig. 37. MRI of 2 and one half year old cervical C4 vertebra axial. (*A*) T1-W and (*B*) FSE T2-W hypointense neurocentral synchondroses (*arrows*).

respect to signal. The cartilage is hypointense, becoming thinner and more difficult to visualize, and comprises 10% to 15% of the vertebral body height. The IVD is rectangular shaped, hypointense on T1-W images and hyperintense on T2-W images, and 20% to 25% of the height of the vertebral body. The posterior elements/spinous processes are the same signal as the vertebral bodies. The neural foramina are ovoid in shape [24,46,63,64].

The spine of a 2- to 3-year-old child can be used as the norm for the pediatric patient. By this time, the normal spinal curvature has developed. The lack of signal from the ossified cortex of the vertebral bodies is seen on all pulse sequences, with some very mild changing in the marrow of the vertebrae producing a slightly high signal on T1-W and FSE T2-W images. The developing slight hyperintensity seen in the vertebrae on the T1-W and FSE T2-W images in infants and young children is felt to be related to some lipid infiltration of the marrow early in life. However, true conversion to fatty marrow appears to be a different process because 80% to 90% of the marrow in young children is red and not yellow (fat) (Figs. 36–38). The neurocentral

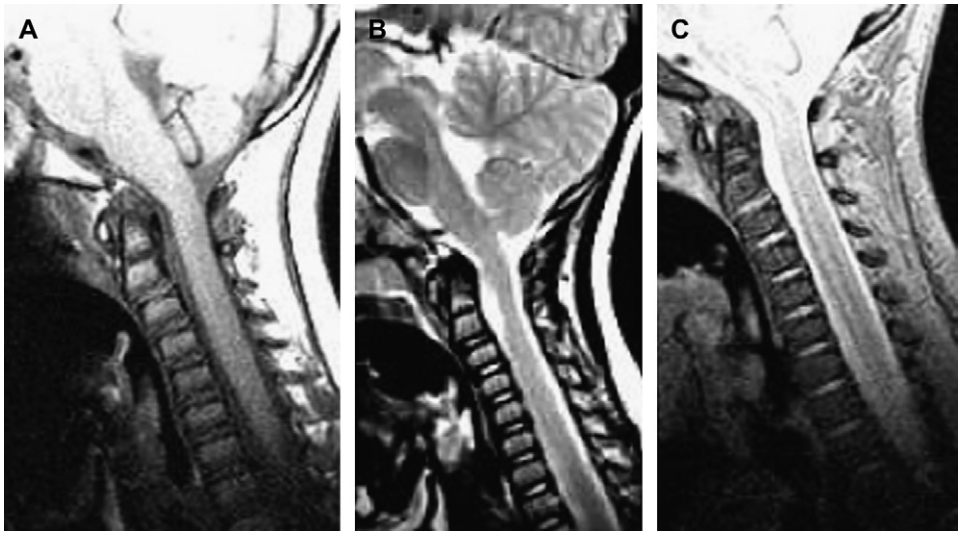

Fig. 38. MRI sagittal images of cervical spine in a 6-year-old. (*A*) T1-W slightly hyperintense vertebrae. (*B*) FSE T2-W slightly hyperintense vertebrae. (*C*) GE T2-W slightly hypointense vertebrae.

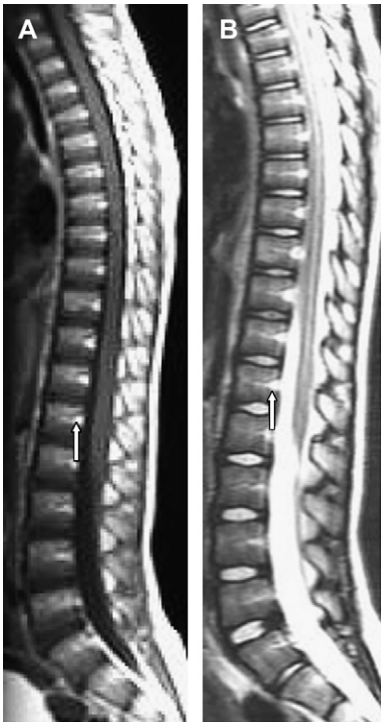

Fig. 39. MRI sagittal images of thoracolumbosacral spine in a 7-year-old. (*A*) T1-W slightly hyperintense vertebrae. (*B*) FSE T2-W slight hyperintense vertebrae. The posterior channel in the midportion of the vertebral body for the basivertebral vein demonstrates hyperintensity (*arrows*).

synchondroses are hypointense on T1-W and FSE T2-W images, and hyperintense on GE T2-W images (see Fig. 32 and 37). The disc is hypointense on T1-W images and markedly hyperintense on T2-W images. The parts of the disc, the annulus fibrosus (outer part) and nucleus pulposus (inner part), may begin to be differentiated by age 5. The anterior artery of the vertebral body can be seen in the newborn and young infant (see Fig. 30). However, the posterior channel with the basivertebral vein can be seen throughout life on some of the different pulse sequences (Fig. 39) [24,46,63,64].

The spinal ligaments demonstrate no signal on either the T1- or T2-W images in all age groups. The T2-W images better demonstrate the ligaments, with easy differentiation of the anterior and posterior spinal ligaments. The ligamentous attachments at the base of the skull with C1 and C2 and the ligamentous attachments of the posterior elements, although demonstrated on MRI, cannot be separated into individual attachments (see Fig. 39; Fig. 40) [7–9,64].

During infancy and childhood, enhancement on MRI using a routine intravenous dose of gadolinium 0.1 mmol/kg or 0.2 mL/kg can be seen in certain structures such as vertebrae and their cartilaginous end plates. In the newborn to children age 2, marked to mild homogeneous enhancement can be seen in the vertebrae (body and posterior elements) (see Figs. 31 and 32). Mild homogeneous enhancement can be seen in

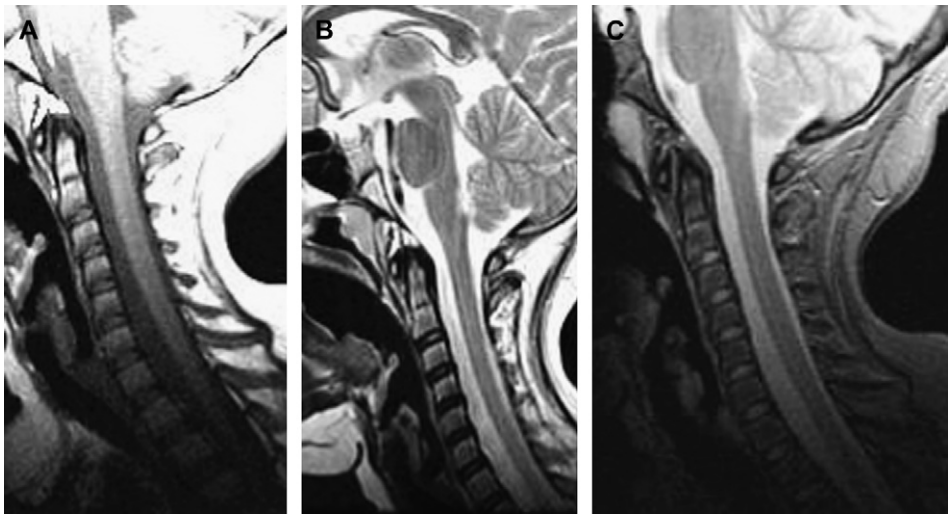

Fig. 40. MRI sagittal images of cervical spine in an 11-year-old. (*A*) T1-W slightly hyperintense vertebrae. (*B*) FSE T2-W slightly hyperintense vertebrae. (*C*) GE T2-W slightly hypointense vertebrae.

the vertebrae from 2 to 7 years of age. No enhancement in the vertebrae should be seen after 7 years of age (Figs. 39 and 40). Enhancement of the hyaline cartilaginous end plates of the vertebral bodies can be seen in the newborn to age 18 months. Enhancement of the basivertebral venous plexus can be seen in all pediatric patients but it is most pronounced in newborns, infants, and young children. The normal IVDs and spinal cord should not demonstrate enhancement on MRI. Enhancement of the vertebrae and cartilaginous end plates are related to their rich vascular supply, the permeability of the endothelium of their capillaries, and their extensive extravascular spaces [65].

References

[1] Weinstein SL, editor. The pediatric spine: principles and practice. 2nd edition. Philadelphia: Lippincott Williams & Wilkins; 2001.

[2] Kirks DR, editor. Practical pediatric imaging: diagnostic radiology of infants and children. 3rd edition. Philadelphia: Lippincott Williams & Wilkins; 1998.

[3] Swischuk LE, editor. Imaging of the newborn, infant, and young child. 5th edition. Philadelphia: Lippincott Williams & Wilkins; 2003.

[4] Kuhn JP, Slouis T, Haller J. Caffey's pediatric imaging. 10th edition. Philadelphia: Elsevier; 2004.

[5] Epstein B, editor. The spine: a radiologic text and atlas. 4th edition. Philadelphia: Lea & Febiger; 1976.

[6] Harwood-Nash DC, Fitz CR. Neuroradiology in infants and children. St. Louis (MO): Mosby; 1976.

[7] Ball WS Jr. Pediatric neuroradiology. Philadelphia: Lippincott-Raven Press; 1997.

[8] Barkovich AJ. Pediatric neuroimaging. 4th edition. Philadelphia: Lippincott Williams & Wilkins; 2005.

[9] Atlas SW. Magnetic resonance imaging of the brain and spine. 3rd edition. Philadelphia: Lippincott Williams & Wilkins; 2002.

[10] Tortori-Donati P, Rossi A. Pediatric neuroradiology brain, head, neck and spine. Berlin: Springer-Verlag; 2005.

[11] Pick TP, Howden R, editors. Gray's anatomy: the anatomical basis of medicine and surgery. 39th edition. Philadelphia: Elsevier Churchill Livingstone; 2005.

[12] Clemente C. Anatomy: a regional atlas of the human body. 5th edition. Philadelphia: Lippincott Williams & Wilkins; 2006.

[13] Sinnatamby CSS, Last RJ. Last's anatomy: regional and applied. 10th edition. Philadelphia: Elsevier; 2000.

[14] Pansky B. Review of Gross Anatomy. 6th edition. New York: McGraw-Hill; 1995.

[15] Byrd SE, Darling CF. Chapter 7: Postnatal maturation of the spine. In: McLone DG, editor. Pediatric neurosurgery surgery of the developing nervous system. 4th edition. Philadelphia: W.B. Saunders Co.; 2001.

[16] Swischuk LE. Emergency imaging of the acutely ill or injured child. 4th edition. Philadelphia: Lippincott Williams & Wilkins; 2000.

[17] Kricun R. Computed tomography. In: Kricun ME, editor. Imaging modalities in spinal disorders. Philadelphia: Harcourt Brace Jovanovich, Inc.; 1988. p. 376–467.

[18] Zimmerman RA, Gibby WA, Carmody RF. Neuroimaging: clinical and physical principles. 1st edition. New York: Springer-Verlag; 2000.

[19] Knollmann F, Coakley FV. Multislice CT principles and protocols. 1st edition. Philadelphia: Saunders-Elsevier; 2006.

[20] Lipson SA. MDCT and 3D workstations: a practical guide and teaching file. New York: Springer; 2006.

[21] Rydberg J, Buckwalter KA, Caldemeyer KS, et al. Multislice CT: scanning techniques and clinical applications. Radiographics 2000;20:1787–806.

[22] Carty H, Brunelle F, Stringer DA, et al. Imaging children. 2nd edition. Philadelphia: Elsevier; 2005.

[23] St. Amour TE, Hodges SC, Laakman RW, et al. MRI of the spine. New York: Raven Press; 1994.

[24] Khanna AJ, Wasserman BA, Sponseller PD. Magnetic resonance imaging of the pediatric spine. J Am Acad Orthop Surg 2003;4(4):797–833.

[25] Byrd SE, Darling CF, McLone DG, et al. MR imaging of the pediatric spine. Magn Reson Imaging Clin N Am 1996;4(4):797–833.

[26] Byrd SE, Fitz CR. Chapter 3: The brain and spine. In: Silverman FN, Kuhn JP, editors. Caffey's pediatric x-ray diagnosis. 9th edition. St. Louis (MO): Mosby. p. 201–343.

[27] McLone DG. Pediatric neurosurgery: surgery of the developing nervous system. 4th edition. Philadelphia: W.B. Saunders; 2001.

[28] Verbout AJ. The development of the vertebral column. Adv Anat Embryol Cell Biol 1998;90:1–122.

[29] Keim H. The adolescent spine. New York: Grune & Stratton; 1976.

[30] Bailey DK. The normal cervical spine in infants and children. Radiology 1952;59:712–9.

[31] O'Rahilly R, Benson DR. The development of the vertebral column. In: Bradford DS, Hensinger RM, editors. The pediatric spine. New York: Thieme; 1985.

[32] Gadow HF. The evolution of the vertebral column. Cambridge University Press; 1933.

[33] Bradner ME. Normal values of the vertebral body and intervertebral disk index during growth. AJR Am J Roentgenol 1970;110:618–27.

[34] Gooding CA, Neuhauser EBD. Growth and development of the normal vertebral body in the presence and the absence of stress. AJR Am J Roentgenol 1965;93:388–94.

[35] Taylor JR. Growth of human intervertebral discs, vertebral bodies. J Anat 1975;120:49–68.

[36] Knutsson F. Growth and differentiation of the postnatal vertebrae. Acta Radiol 1961;55:401–8.
[37] Ford DM, McFadden KD, Bagnall KM. Sequence of ossification in human vertebral neural arch centers. Anat Rec 1982;203:175–8.
[38] Ogden JA. Radiology of postnatal skeletal development: XI. The first cervical vertebra. Skeletal Radiol 1984;12:12–20.
[39] Ogden JA. Radiology of postnatal skeletal development: XII. The second cervical vertebra. Skeletal Radiol 1984;12:169–77.
[40] Brill PW, Baker DH, Ewing ML. "Bone-within-bone" in the neonatal spine: stress change or normal development? Radiology 1973;108:363–6.
[41] Ebel KD, Blickman H, Willich E, et al. Differential diagnosis in pediatric radiology. New York: Thieme; 1999.
[42] Lustrin ES, Karakas SP, Ortiz AO, et al. Pediatric cervical spine: normal anatomy, variants, and trauma. Radiolographics 2003;23:539–60.
[43] Overton LM, Grossman JW. Anatomical variations in the articulation between the second and third cervical vertebrae. J Bone Joint Surg [Am] 1952;34: 155–61.
[44] Catell HS, Filtzer DL. Pseudosubluxation and other normal variations in the cervical spine in children. A study of one hundred sixty children. J Bone Joint Surg [Am] 1965;47:1295–309.
[45] Jacobson G, Leecker HH. Pseudosubluxation of the axis in children. AJR Am J Roentgenol 1959;82: 472–81.
[46] Sze G, Baierl P, Bravo S. Evolution of the infant spinal column: evaluation with MR imaging. Radiology 1991;181:819–27.
[47] Silverman FN, Kuhn JP. Introduction to the spine. In: Caffey's pediatric x-ray diagnosis: an integrated imaging approach. St. Louis (MO): Mosby; 1993. p. 116–25.
[48] Simril WA, Thurston D. Normal intrepediculate space in the spines of infants and children. Radiology 1955;64:340–7.
[49] Markuske H. Sagittal diameter measurements of the bony cervical spinal cord in children. Pediatr Radiol 1977;6:129–31.
[50] Hinck VC, Clark WM Jr, Hopkins CE. Normal interpediculate distances (minimum and maximum) in children and adults. AJR Am J Roentgenol 1966;97:141–53.
[51] Hinck VC, Hopkins CE, Savara BS. Sagittal diameter of the cervical spinal canal in children. Radiology 1962;79:97–108.
[52] Hinck VC, Hopkins CE, Clark WM. Sagittal diameter of the lumbar spinal cord in children and adults. Radiology 1966;85:929–37.
[53] Yousefzadeh DK, El-Khoury GY, Smith WL. Normal sagittal diameter and variation in the pediatric cervical spine. Radiology 1982;144:319–25.
[54] Naik DR. Cervical spinal canal in normal infants. Clin Radiol 1970;21:323–6.
[55] Schwarz GS. Width of spinal canal in growing vertebra with special reference to sacrum; maximum interpediculate distance in adults and children. AJR Am J Roentgenol 1956;76:476–86.
[56] Elsberg CA, Dyke CG. Diagnosis and localization of tumors of spinal cord by means of measurements made on x-ray films of vertebrae and the correlation of clinical and x-ray findings. Bull Neurol Inst New York 1936;3:359–69.
[57] Landmesser WE, Heublein GW. Measurement of the normal interpedicular space in the child. Conn Med 1953;17:310–3.
[58] Brookes M. The blood supply of bone: an approach to bone biology. New York: Appleton; 1971.
[59] Crock HV, Yoshizawa H. The blood supply of the vertebral column and spinal cord in man. New York: Springer-Verlag; 1977.
[60] Dooms GC, Fisher MR, Hricak H, et al. Bone marrow imaging: magnetic resonance studies related to age and sex. Radiology 1985;155: 429–32.
[61] Vogler JB III, Murphy WA. Bone marrow imaging. Radiology 1988;168:679–93.
[62] Ricci C, Cova M, Kang YS, et al. Normal age-related patterns of cellular and fatty bone marrow distribution in the axial skeleton: MR imaging study. Radiology 1990;177:83–8.
[63] Sebag GH, Dubois J, Tabet M, et al. Pediatric spinal bone marrow assessment of normal age-related changes in the MRI appearance. Pediatr Radiol 1993;23(7):515–8.
[64] Walker HS, Dietrich RB, Flannigan BD, et al. Magnetic resonance imaging of the pediatric spine. Radiographics 7(6):L1129–52.
[65] Sze G, Bravo S, Baierl P, et al. Developing spinal column: gadolinium-enhanced MR imaging. Radiology 1991;180(2):497–502.